

https://dspace.org/

Synthesis of Eudragit RL-100 and Pluronic F127 nanoparticles for the oral delivery of Ampicillin

Van Rooyen, H P

2021

https://hdl.handle.net/10539/33498

Downloaded from a DSpace repository. https://dspace.org/

SYNTHESIS OF EUDRAGIT RL-100 AND PLURONIC F127 NANOPARTICLES FOR THE ORAL DELIVERY OF AMPICILLIN

HP VAN ROOYEN



A research report submitted to the Faculty of Health Sciences, University of the Witwatersrand,
in partial fulfilment of the requirements for the degree of
Master of Science MSc (Med) Pharmaceutical Affairs Part-time

Supervisors

Professor Pierre P. D. Kondiah
University of the Witwatersrand, Department of Pharmacy and Pharmacology, Johannesburg, South Africa, 2020

Professor Yahya E. Choonara
University of the Witwatersrand, Department of Pharmacy and Pharmacology, Johannesburg, South Africa

DECLARATION

I, Henro Patrie van Rooyen declare that this research report is my own. This work is a submission for the degree of Master of Science in Medicine (MSc (Med)) part time in the field of Pharmaceutical Affairs to the Faculty of Health Sciences as a research component at the University of Witwatersrand, Johannesburg. It has not been submitted for examination before for any degree at this or any other University.



10 Aug 2021

…… ……

Name Signature Date

DEDICATIONS AND ACKNOWLEGDEMENTS

Nothing in life comes without hard work, dedication and extreme persistence. Everyone wants success, but not everyone is willing to do the hard work required to reap those benefits. To my wife, Lizerie van Rooyen, you are my absolute rock and the place where I feel at ease. To a lifetime of joy ahead.

Thank you to Accelerated Enrollment Solutions (Synexus) for the financial and structural support and allocated off time work to conduct my laboratory experiments and attend evening lectures.

I would like to acknowledge and thank Prof. Yahya Choonara and Prof. Pierre Kondiah extensively for their continuous assistance, patience, and guidance during laboratory work and final write up, as well as the Thuthuka grant of Prof. Kondiah for the funding of this project. Also – the tireless work of the laboratory technical support staff is highly appreciated. Those members include: Mr. Sello Ramarumo, Mr. KB Mohlabi and Mr. Bafana Themba.

Lastly, the passing of Prof Viness Pillay has left a vacuum in the department. His presence will be missed daily, may his sole rest in peace.

Dream do not work unless you do.

ABSTRACT

Industry leaders along with the World Health Organisation (WHO) are suggesting that the biggest threat to human health, and the reservation will come from what is deemed currently as antimicrobial drug resistance. With anti-microbial resistance being on the rise, it is imperative that large pharmaceutical companies allocate adequate financial resources towards the development of new anti-microbial agents. This is due to global slow economic growth and previously observed low return on investment (ROI) on developing these molecules ROI is more favoured to other therapeutic areas such as chronic ambulatory diseases. These two factors accentuate the problem that modern medicine in this indication will face soon. Innovative and unique methods for resolving this imminent thread mankind faces are desperately needed.

Advance drug delivery platforms can be utilised to overcome previous issues identified in anti-microbial treatment using mainstay oral dosing. These issues include low bio-availability, sub-optimal plasma concentrations, extensive first pass metabolism and toxicity leading to adverse drug reactions and associated severe side effects. All these issues have and are currently hindering the adequate treatment of non-superficial bacterial infections to achieve adequate and efficacious blood plasma concentrations for effective microbe eradication. This study was aimed at enhancing the physicochemical properties and dosing guidelines of previously excessively prescribed anti-microbial agents (such as β-lactams) employing nanoparticle technology. It is hypothesized that enhancing this drug class' delivery, will increase its current non-optimal physicochemical properties and dosing strategy. Various physicochemical experiments were conducted on nanoparticles (NP) consisting of Eudragit RL-100 and surfactant Poloxamer encapsulating ampicillin anhydrous as model drug. In this current study both the AMP-load Eudragit and Pluronic® F-127 NPs and the mainstay drug (Ampicillin) saw an initial spike in release in simulated gastric pH with a total offload percentage of 9.57% and 7.70% respectively in the first 30 min post dose.

There was however an increase of roughly 0.5% - 1.7% of additional drug off-loaded earlier from the nanoparticulate system following an oral formulation as compared to mainstay drug. Furthermore, drug encapsulation efficacy was equated at 66%. The study's key finding indicated that compared to baseline (traditionally dosed oral ampicillin) the release profile of ampicillin loaded within polymers illustrated a more sustained release in simulated gastrointestinal pH profiles with that would possibly result in a higher initial drug offload amount increasing plasma-drug concentration.

Keywords: Anti-microbial resistance, bioavailability, advance drug delivery platforms, pharmacokinetic testing, drug encapsulation, personalised medicinal dosing, nanoparticles, polymers

TABLE OF CONTENTS

DECLARATION……ii

DEDICATIONS AND ACKNOWLEDGMENTS……iii

ABSTRACT……iv

TABLE OF CONTENTS……vi

LIST OF FIGURES……vii

LIST OF TABLES ……ix

LIST OF EQUATIONS……x

LIST OF ABBREVIATIONS……xiii

CHAPTER 1 ……1

CHAPTER 2……7

CHAPTER 3……25

CHAPTER 4……32

CONCLUSION AND FUTURE RECOMMENDATIONS……51

REFERENCES ……55

APPENDIX A ……68

APPENDIX B ……69

LIST OF FIGURES

Figure 1-1: Schematic showing the role of lipophilicity in boosting cellular uptake of small drug molecules. Generally, when small molecules cross lipid bilayer by simple diffusion, they firstly accumulate in the hydrophobic regions of the lipid bilayer at high concentration through hydrophobic interaction (Hoshyar, 2016) (Permission received for reproduction).

Figure 2-1: Typical timeline showing the introduction of an antibiotic and the development of clinically significant resistance. Adapted with permission (Linlin, 2017).

Figure 2-2: Oral delivery routes for drug-loaded nanopolymer and nano lipid structures. An Illustration utilising Chitosan as nanoparticle delivery mechanism. (Safhi, 2016) (Permission received for reproduction).

Figure 2-3: Multiple mechanisms of antimicrobial action of nitric oxide-releasing nanoparticles (NO NPs), chitosan-containing nanoparticles (chitosan NPs), silver-containing nanoparticles (Ag NPs), zinc oxide-containing nanoparticles (ZnO NPs), copper-containing nanoparticles, titanium dioxide-containing nanoparticles (TiO2 NPs), and magnesium-containing nanoparticles (Yang, 2018) (Permission received for reproduction).

Figure 3-1: Calibration curve showing the relationship between ampicillin concentration in PBS and absorbance.

Figure 4-1: Visualization of the AMP-loaded EU-RL-PF127nanostructure using SEM.

Figure 4-2: FTIR Results. A) Pluronic® F-127, B) Ampicillin Free drug C) Distinction shown between the two NP (blank C-1 and Loaded C-2).

Figure 4-3: Typical particle size distribution to establish the mean particle size of A) Blank NPs and B) AMP-loaded NPs.

Figure 4-4: Zeta potential profiles of A) AMP-loaded NPs with a value of -0.319 ± 0.7 mV and B) blank NPs with a value of -23.3 ± 2.7 mV.

Figure 4-5: DSC curves of AMP (A). Eudrigit RL100 – Pluronic® F-127 nanoparticles (Blank) (B) and AMP-loaded Eudrigit RL100 – Pluronic® F-127 nanoparticles (C).

Figure 4-6: Physical stability kinetics of the NPs, a) AMP-loaded NPs, b) Blank NPs and c) native AMP. Data indicates the ΔBS and T measured at 25 ± 0.5°C at 5 minute intervals, over a 1 hour duration.

Figure 4-7: Percentage of AMP drug released from Eudragit and Pluronic® F-127 NP in simulated gastric pH environment.

Figure 4-8: Percentage of AMP drug released from loaded NP dosed within a gelatin hard capsule against base AMP in various simulated gastric pH environments.

Figure 4-9: 10 mg Blank-NPs and 10 mg AMP-loaded NPs illustrated in a MIC plate. Columns 1,2 and 3 contained 10 mg of loaded NP and columns 4,5 and 6 houses the 10 mg blank NPs. Columns 7 and 8 were the culture control *Staphylococcus aureus* (ATCC#25923). Columns 10 was Acetone and 11 drug control (10 mg of ampicillin anhydrous). The 10 mg NPs showed a significant inhibition during their serial dilutions in all rows, concluding that this concentration illustrates complete inhibition.

LIST OF TABLES

Table 2-1: Developed defense mechanisms microbes employ against antimicrobial agents.

Table 2-2: Some representative antibiotics, their modes of action and mechanisms of resistance.

Table 4-1: Minimum Inhibitory Concentrations (MIC) values obtained during experimentation to determine the antimicrobial efficacy of two different quantities of NPs.

LIST OF EQUATIONS

Equation 1: Determination of drug entrapment efficiency (EE%) utilizing linearity graph $R^2 = 0,9787$

Equation 2: Loading and entrapment efficiency of AMP into Eudragit RL 100 nanoparticles

APPENDIX A

Table 4-1. Table illustrating both PDI and zeta potential values of blank AMP and AMP-loaded NPs.

Table 4-2: Percentage release of drug within NP and drug contained within the Gelatin delivery system comparison. Note the stark distinction at 180 min for AMP-load Eudragit and Pluronic® F127 NP and Ampicillin capsules.

APPENDIX B

Figure 4-10: Simple disc diffusion of pathogen *S. aureus #25923*. Disc's loaded with NP (1 mg) for 30 sec. Cultured overnight for 24hrs at 37 °C.

Figure 4-11: Simple disc diffusion of pathogen *S. aureus #25923*. Disc's loaded with NP (10 mg) for 30 sec. Cultured overnight for 24 hrs at 37 °C.

LIST OF ABBREVATIONS

3D	- Three Dimensional
2D	- Two Dimensional
ADC	- Antibody drug conjugate
AMP	- Ampicillin
AMR	- Antimicrobial drug resistance
AZM	- Azithromycin
API	- Active pharmaceutical ingredients
CLR	- Clarithromycin
Cmax	- Maximum plasma concentration
DSC	- Differential Scanning Calorimetry
DEE%	- Encapsulation efficiency
EPS	- Extracellular polymeric substance
FTIR	- Fourier-transform infrared spectroscopy
GIT	- Gastro-intestinal tract
IM	- Intramuscular Injection
MBC	- Minimum bactericidal concentration
MIC	- Minimum inhibitory concentrations
MPS	- Mononuclear phagocyte system
MOA	- Mechanism of action
NP	- Nanoparticle
NL	- Nanoliposome
Nm	- Nanometer
NS	- Nanosystem
NDM-1	- New Delhi metallo - ß-lactamase-1
NRU	- Neutral Red Uptake (NRU)
NO NP	- Nitric oxide-releasing nanoparticles
PABA	- Para-aminobenzoic acid
PDI	- Polydispersity Index
PLC	- Polycaprolactone
PLGA	- Poly(lactic-co-glycolic acid)
PVA	- Polyvinyl alcohol

QAC - Quaternary ammonium compounds
R&D - Research and development
RNOS - Reactive nitrogen oxide intermediates
ROI - Return on Investment
SGF - Simulated gastric fluid
SEM - Scanning Electron Microscopy
SIF - Simulated intestinal fluid
SLNR - Solid Lipid Nanoparticle-Based
TA - Toxin – Anti toxin
TSA - Tryptone Soya agar
WHO - World Health Organization
ΔBS - Delta Backscattering
π-π - Pi – Pi

CHAPTER 1
INTRODUCTION

1.1 Introduction

Orme (1984) reported that there are various factors that complicate the oral dosing of anti-microbial drugs (antibiotics) from a pharmacokinetic and pharmacodynamic perspective. At that time, there was already a robust and focused discourse on biopharmaceutics and its role in the design of medicines with it being described as ‘’the study of the influence of pharmaceutical formulation on the *in vivo* performance of a drug’’. Nearly 30 years later modern medicine still conforms to this principle.

In the last two decades, the development of novel antibiotics has not been given much impetus by multinational pharmaceutical companies due to the increasing challenges faced with undertaking clinical trials in this therapeutic area. Inappropriate study designs and an increase in patient adverse events during clinical trials are the most prominent setbacks (Helen, 2013). The loss of antibiotic effectiveness, largely due to microbial drug resistance further adds to the dilemma. Acute infection-induced pathophysiological changes such as organ dysfunction and increased capillary permeability are known to lead to alterations in antibiotic volume of distribution and clearance (Blot, 2014). Furthermore, an effect on absorption and first pass effect cannot be ruled out in advance, as possible perfusion or other yet unknown alterations to the gastrointestinal tract may be present during the acute phase of microbial infection (Roberts, 2013).

Historically, dosing anti-microbial drugs orally have been difficult due to the various different physiological challenges they are to overcome *in vivo*. Orally administered antibiotics must undergo absorption from the gut and first pass metabolism before entering the systemic circulation, often causing a bioavailability of significantly less than 100%, resulting in delayed and lower maximum concentrations in blood and at the site of infection compared to other parenteral dosing regimens, such as IV administration (Jager, 2016).

Nanosystems (NS) may enhance oral absorption by increasing the gastric residence time through mucosal adhesion or by increasing cell or tissue entry (e.g., Peyer's patches and M cell-mediated uptake) (Florence, 2005). Other factors that contribute to prolonging particle and drug circulation times of nanoparticle molecules are, modulation of mechanical properties, engineering particle morphology and hitchhiking on red blood cells (Yoo, 2010). All of these aforementioned properties positively influence the absorption of nanoparticles and increases the bioavailability of the carried drug molecule loaded within.

Therefore, immediate interventions to mitigate the risk of inefficient antibiotic therapy are urgently required. This includes the need to develop new antibiotics and advanced drug delivery systems to enhance the bioavailability of existing antibiotics. In addition, there is also an increase in antibiotic resistant microbes that poses the biggest risk (Grogan, 2019). Ampicillin (AMP) is a molecule that is more than 90 years old and still used regularly to treat bacterial infections. It is prescribed in the treatment protocol regime for invasive Group A *Streptococcal* infection (Levison, 2009). AMP inhibits the activity of enzymes that are needed for the crosslinking of peptidoglycans found in the bacterial cell wall required for the final step in the biosynthesis pathway for adequate cell wall synthesis of bacteria (Yocum, 1990). Currently, AMP has a poor bioavailability with only 30% absorbed from the small intestine under optimal conditions after oral administration. Due to its susceptibility to acid hydrolysis, oral doses are normally excessive and dosed at 4-5 times greater to what would be an equivalent Intramuscular dose. In addition, the half-life of AMP is recorded at 30-60 minutes after oral dosing (Gilman, 1990).

Majority of bacterial infections occur at infection sites outside the bloodstream, where antibiotic tissue concentrations are of significant relevance to optimize treatment. The more frequently prescribed antibiotics are extremely hydrophilic and unable to penetrate through the lipid membranes of infected cells (Baietto, 2014). Delivering such drugs to the site of infection that is usually located within fatty tissue or around an implanted device where microbial pathogenic biofilms develop is critical to ensure that the infection can be cleared without the need for additional interventions (such as surgery or prolonged treatment) (Turosa, 2007).

Uncontrolled diffusion of antibiotics within infected tissue/cell is another contributing factor resulting in systemic side effects (Lagler, 2014). The research conducted within is to assist in further discovery of possible dosing regimens (via altering drug-and-delivery molecule physicochemical makeup) to maximize clinical benefit while minimizing the risk of toxicity. The use of polymeric drug delivery strategies has the potential to overcome these challenges. Previous research has demonstrated the use of a variety of different molecules (including β-lactam drug molecules) loaded within polymeric frameworks to provide spatio-temporal drug delivery can be beneficial (Mahapatro, 2011). By analyzing the structural and physicochemical properties of the nanosystem, the possibility of administering AMP in lower doses via the oral route would exist resulting in a reduction in side effects and contribute to overcoming antibiotic resistance. By utilizing more lipophilic polymers site-specific delivery of antibiotics can be achieved (Turosa, 2007). Figure 1.1 below illustrates visually how lipophilicity enhances cellular absorption of small drug molecules utilizing nanotechnology.

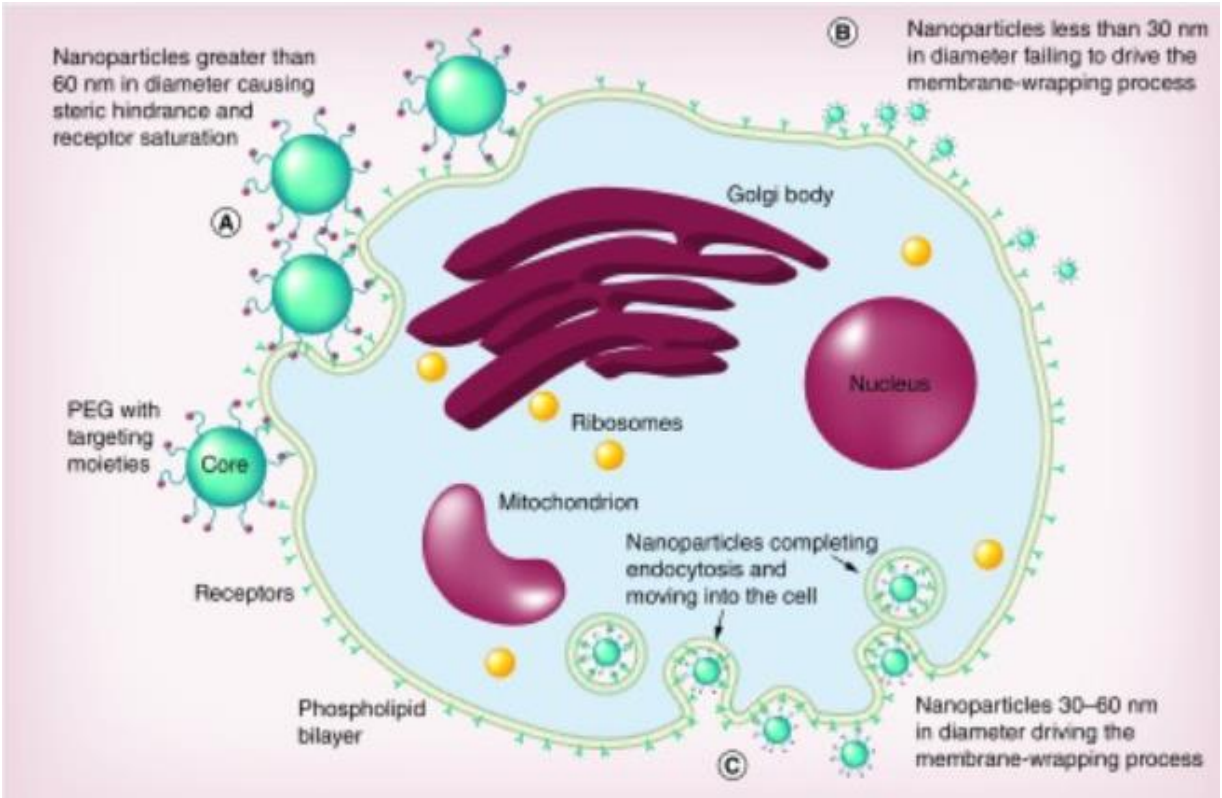

Figure 1-1: Schematic showing the role of lipophilicity in boosting cellular uptake of small drug molecules (Hoshyar, 2016) (Permission received for reproduction).

1.2 Rational and Motivation of this Study

Current conventional oral antibiotic prescriptions under primary healthcare practitioners are non-targeted and therefore result in undesirable side effects, erratic plasma concentrations and sub-therapeutic drug levels. Antibiotics are also known to further disrupt the normal body flora (microbiota) which is required to sustain body-homeostasis (Chifiriuc, 2016). There has been extensive research in the field of nano-enabled antibiotic therapy that renders this approach viable. Nanoconstructs such as nanoliposomes (NLs) and polymeric nanoparticles (NPs) have been explored (Fernando, 2018). This strategy can also assist in combating antibiotic drug resistance by ensuring appropriate plasma levels of drug are available at the site of bacterial infection (Pawar, 2014). Therefore the rationale of this study was to use polymer blends comprising polymethylmethacrylate (PMMA) and PEG-PPG-PEG as a surfactant to increase the bioavailability of model drug AMP loaded into NPs whilst also assisting in reducing resistance buildup.

1.3 Aim and Objectives of this study

The main aim of this study was to design, develop and evaluate the use of nanoparticles (NPs) to improve the oral delivery of the model antibiotic ampicillin. Secondary endpoints explored were to resolve the solubility challenges of AMP and increase its intestinal absorption.

In order to achieve this aim the following objectives were completed:

1. Synthesis of polymeric nanoparticles comprising PMMA and PEG-PPG-PEG for AMP-loading as an orally administered drug delivery system.
2. Undertook detailed physicochemical characterization of the nanosystem that included particle size and zeta potential measurements, morphological evaluation via SEM, assessment of the chemical structure integrity and composition using Fourier Transform Infrared spectroscopy, assessment of the thermal stability via Differential Scanning Calorimetry (DSC).

3. Undertook *in vitro* drug release testing of the native AMP-loaded nanosystem and within a gelatin capsule to explore the pattern of drug release over a period of 2.5 hours in simulated gastric fluid (SGF) and for 24 hours in simulated intestinal fluid (SIF).
4. Determined the antibacterial properties of the new nanosystem using different polymers against the current standard of care in oral form.

1.4 Overview of this Research Report

Chapter One: Provides an introduction to the Research Report as well as highlighting the importance and etiology of antibiotic resistance. A concise discussion on how nano-enabled drug delivery systems can be a utilized as an advanced solution to surmount the challenges of poor bioavailability and contribute to alleviating antibiotic resistance. The rationale, motivation, aim and objectives of the study is also outlined**.**

Chapter Two: Presents an assimilation of the previous pertinent literature focusing on the current study undertaken in the fields of drug delivery and nanomedicines related to antibiotic resistance. This Chapter also summarizes the mechanisms of antibiotic drug resistance and further highlights the use of nanoparticles to enhance antimicrobial action.

Chapter Three: Comprehensively describes the synthesis and development of the AMP-loaded nanosystem utilizing a previous described form of nanoprecipitation.

Chapter Four: Reports and discusses the *in vitro* findings and results obtained from the various physiochemical experiments undertaken. It discusses the AMP entrapment efficiency within the nanosystem, the comparative drug release behavior (nanosystem vs. conventional system) and the antimicrobial efficacy of the nanosystem through evaluation of the MIC values.

Future recommendations: Provides a recommendation for future work related to this study and potential adaptations that can be incorporated to further enhance the nanosystem to combine a variety of other β-lactam antibiotics using two different techniques that can add further value to the current study as a future perspective. It also suggests additional *in vitro toxicology* and *in vivo* pharmacokinetic studies to be incorporated to explore toxicological characteristics and biological effects, respectively.

CHAPTER 2

A LITERATURE REVIEW OF NANO-ENABLED DRUG DELIVERY SYSTEMS FOR THE ORAL ADMINISTRATION OF ANTIBIOTICS

2.1. Introduction

For the past few decades industry leaders along with the World Health Organisation (WHO) have suggested that the biggest threat to human health will come from antimicrobial drug resistance (AMR). The issue of AMR has been increasing since the dawn of antibiotic molecules. At that stage, a strong correlation already existed between the amount of antibiotics used in total circulation (agriculturally and medically) and resistance build up.

The quantity of antibacterial molecules in phase II or III clinical trials remains alarmingly low. The tempo of research and development (R&D) in this field must accelerate and increase drastically to keep up with the possible negative health implications and consequences that bacterial resistance brings along (Boucher, 2013). Due to the current unfavourable economic climate, large pharmaceutical companies would rather invest their money elsewhere such as chronic ambulatory diseases, which favours a more sustainable clientele requiring regular dosing as with any chronic disease or frequently occurring acute infection. Developments in new antimicrobial agents have been scarce and more innovative solutions to the pressing and imminent issues regarding resistance build-up are desperately needed (Prestinaci, 2015).

Nanotechnology has been a topic of interest for a while in possibly aiding to alleviate this pressing challenge of AMR. Nano-enabled drug delivery systems has been receiving significant attention due to the favourable pharmaceutical and pharmacological characteristics that include, but is not limited to, a favourable pharmacokinetic profile, ease of manufacturing and possible ad-hoc adaptations to increase the effortlessness of individual patient profiling and importantly adequate dosing amounts (Cerqueira, 2017).

Due to distinctive physicochemical characteristics, NPs are susceptible and selective in detecting bacterial signals and may exhibit as a result their intrinsic antimicrobial properties (Li, 2018). In addition, due to certain unique physiological properties, NPs may be used for the delivery of antimicrobial drugs, which can resist microbial adhesion and contamination. These specifics are instrumental in compromising the distinct defense pathways of bacteria to antimicrobial resistance (Hajipour, 2012).

Nano-enabled drug delivery systems can offer an improved strategy for increasing the therapeutic index and decrease the dosage and frequency of administering antibiotics. In addition, NPs enhance the delivery of intracellular drugs, reduce the possible further production of drug-resistant bacteria and enable very precise targeted organ accumulation of the antimicrobial agent by functionalized surface modifications, resulting in systemic side effects and immunosuppression being restricted (Yeh, 2020). However, despite these promising initial outcomes, the few main challenges of establishing clinical use is related to the evaluation of interactions of nano-antibiotics with cells, tissues and organs achieving information about their possible toxic effects, together with the feasibility of production on a large macroeconomic scale (Abo-Zeid, 2020). Several types of NPs (organic and inorganic) have shown potential in the pharmaceutical field as well as have been studied extensively as potential drug carriers with applications in the delivery of antimicrobial molecules (Blecher, 2011).

This Chapter provides a concise incursion into the concern of AMR by outlining the contributing factors and how the use of advanced nano-enabled drug delivery systems can provide a solution to combat AMR. The mechanisms by which NPs combat AMR are discussed considering recent innovations that include the use of lipid NPs, smart responsive materials and natural compounds.

The chapter also describes recent advances in the development of new oral nanosystems to improve the bioavailability of antibiotics to surmount antibiotic resistance via mechanisms of reduced uptake and Increased drug efflux from the bacterial cell; expression of resistance genes that encode the modified form of the substrate on which the antibiotic attaches and the covalent modification of the antibiotic molecule that inactivates its antimicrobial function. Discussed in the third chapter of this study.

2.2. Specific Mechanisms of Antimicrobial Drug Resistance

The discovery of penicillin in the early 20th century has drastically decreased mortality and morbidity rates unequivocally to anything else as seen in medicine before. Due to the development and increase of anti-microbial resistant bacteria later during this century (as seen in Figure 2-1), the initial outlook has changed. The WHO has identified antimicrobial drug resistance (AMR) as one of the key focus areas of concern for the preservation of human health in the 21st Century (Paterson, 2016). There are, however, various factors that contributes to the bleak picture the WHO has painted. Almost all fields of medicine depends heavily on effective antimicrobial drugs such as; organ transplantation, various surgeries, intensive care for pre-term new-borns and many other medical interventions (Prestinaci, 2015).

Drug resistance can occur as follows:

1. Bacteria acquire resistant genes
2. Resistant genes are then expressed

Bacteria develop resistance to single and multiple drugs by horizontal gene transfer through transformation, conjugation, and transduction, as well as uncontrolled mutation of specific genes (Böhm, 2020). Multi-drug resistance (MDR) is achieved by a bacterial cell that already possesses one drug resistance gene (Qiu, 2012).

Microbes express certain immune orientated genes in response to antibiotic exposure. As a result, resistance becomes more prevalent when microbes that exhibit these specific antibiotic resistance genes increase in circulation due to sub optimal antibiotic exposure and not complete eradication (Zhan, 2019).

In settings that exacerbate selective pressure, the possibility of drug resistance increases, and this includes scenarios of poor patient compliance to antibiotic therapy or the use of time-dependent antibiotics with long half-lives or formulations with poor bioavailability such as β-lactam.

Concentration-dependent antibiotics such as aminoglycosides have clinical outcomes that are functions of the ratio of the maximum drug concentration (C_{max}) per dosing interval to the Minimum Inhibitory Concentration (MIC) (Pelgrift, 2013).

One of the mechanisms anti-microbial drug resistance occur is via sub optimal concentration-dependent exposure to antibiotics medication. This occur when plasma concentration of drug is > 0 while the Cmax/MIC ratio falls below therapeutic index (Liu, 2020). Microbes utilize numerous mechanisms of resistance to antimicrobial drugs as listed in **Table 2-1.**

Table 2-1: Developed defense mechanisms microbes employ against antimicrobial agents.

Reduced uptake and enhanced efflux of drugs from microbial cells (Blasco, 2019).	Expression of resistance genes that code for a modified substrate version to which the antimicrobial agent binds (Torres-Barcelo, 2019).
’Covalent alteration of the bacterial cell's structure inactivates antimicrobial drug molecule binding leading to an increase in antimicrobial drug dysfunction (Lied, 2012).	The development of biofilms can result in bacterial resistance at very high concentrations of many different types of antibiotics, resulting in persistent infections despite antibiotic treatment (Penesyan, 2020).
Synthesis of a molecule that is a competitive inhibitor of the antibiotic (Li, 2018)	Drug tolerance of metabolically inactive persisters (Nurit-Beyth, 2015).
Amplified production of a competitive inhibitor of antibiotic (Friedman, 2008)	Swarming as another mechanism of antibiotic tolerance (Gou, 2020)

The direct link between an overabundance of antimicrobial agents in circulation and the build-up of resistance has also been closely observed as early on as the 50s and 60s. Interestingly, the first stain of Multi-drug resistant *Staphylococcus Aureus* was observed as early on as the 1960 (World Health Organization, 2013). Over prescription

is and for the foreseeable future will be a major player in mitigating the battle against AMR. Large amounts of antimicrobial agents are used in the non-human related scientific industries. Food growth worldwide consumes various antimicrobial agents. These antimicrobial molecules are used in human medicine as well with examples such as gentamycin and streptomycin being the most prominent (Stockwell, 2012). Targeted administration of antimicrobials faces various transport and physiological barriers unique to different organs, tissues and subcellular compartments within microbes when dosed *in vivo* (Gao, 2018). Most mainstay and regularly utilised antibiotic medicines are hydrophilic and unable to spontaneously cross the plasma membrane of the infected cells and localise intracellulary which renders the standard treatment of intracellular infections ineffective (Baietto, 2014).

Traditional and currently used antibiotics extort their mechanism of action by three ways namely, translational machinery, DNA replication machinery and cell wall synthesis inhibitory machinery. Heredity systems that constitutes to AMR are bacterial influx-efflux system, chemical alternations of antibiotics *in vivo* and the alternations of chemical bacterial target molecules that undergoes alternations (Gillings, 2018).

These are strongly associated to genetical factors and the transfer of genes across different organisms/species are well recorded when researching AMR (Linlin, 2017). As such resistance can be divided into intrinsic resistance and acquired resistance according to the source of the resistance genes. Other physiological systems aiding in AMR are; persistence, biofilms and swarming (Jayaraman, 2009). Furthermore - the advanced discovery of gene New Delhi metallo-ß-lactamase-1 (NDM-1) contributed significantly to understanding AMR. These are summarised in Table 2-2.

Table 2-2: Some representative antibiotics, their modes of action and mechanisms of resistance

Category	**Some Members**	**Mode of Action**	**Major mechanisms of resistance**
β-lactam	Penicillins, Cephalosporins, Cefotaximes and Carbapenems	Inhibition of cell-wall synthesis	Cleavage by β-lactamases, CTX-mases, Carbapenemases
Aminoglycosides	Streptomycin, Gentamycin, Tobramycin and Amikacin	Inhibition of protein synthesis	Enzymatic modification, efflux, ribosomal mutations, 16S rRNA methylation
Quinolones	Ciprofloxacin, Ofloxacin and Norfloxacin	Inhibition of DNA replication	Efflux, modification, target mutations
Glycopeptides	Vancomycin	Inhibition of cell-wall synthesis	Altered cell walls, efflux
Tetracyclings	Tetracycline	Inhibition of translation	Mainly Efflux
Oxazolidinones	Linezolid	Inhibition of formation of 70S ribosomal complex	Mutations in the 23S rRNA genes followed by gene conversion

2.3. The Economic impact on the Development of AMR

The decrease in R&D spend by multinational pharmaceutical companies as a result of poor economic conditions is a contributing factor to the AMR epidemic. The decline in investing in new antibiotic research has been hampered by uncertainty of drug development lifecycles from Phase I to Phase IIa / IIb, thus rendering this an unattractable investment option (Li, 2018). R&D to mitigate AMR will have to be led collectively from within a country's policy makers at medicine regulatory institution level.

Tax-rebates are a possible solution to making it worthwhile for a pharmaceutical company to start spending scarce resources in this area of need. This is also one of the current strategies that exist when diverging pharmaceutical companies explore different treatments for orphan drugs. The number of new antibiotics in development are likely too small to withstand and mitigate the increasing rates of bacterial resistance (Savic, 2018). New market models are needed that reward innovation in antibiotic drug development and provide a stronger return on investment for pharmaceutical companies still operating in this space. While rewarding innovation, these models should also promote stewardship of new antibiotics and ensure access to all patients that need them (Li, 2018).

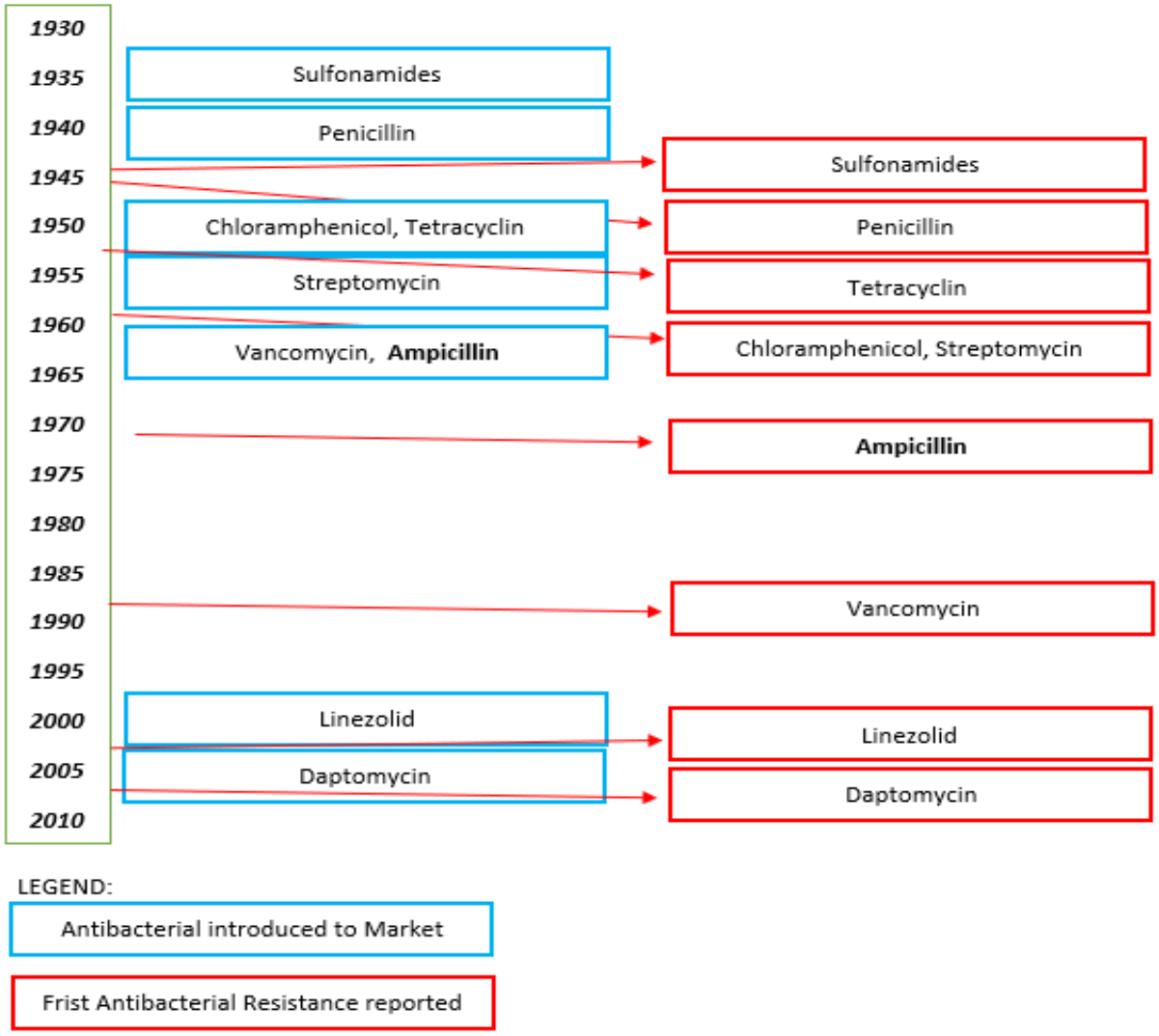

Figure 2-1: Typical timeline showing the introduction of an antibiotic and the development of clinically significant resistance. Adapted with permission (Linlin, 2017).

2.4. Nano-Enabled Drug Delivery Systems to Combat AMR

There are various reasons and postulation about what exactly constitutes AMR. One of the recurring issues is the non-optimal or non-effective dosing techniques used to eradicate infection effectively and efficiently. Traditional treatment regimens are effective however, not optimal. Hence, formulation optimization is desperately needed (Aliabadi, 2000).

One of the main paradigm shifts in the pharmaceutical sciences is the use of nanotechnology to produce nanomedicine (Rantanen, 2015). With this area of advanced nano-enabled drug delivery explored regularly, scientific breakthroughs in finding easier and more efficient ways of producing nanoparticles (NPs) at lower cost will make the possible incorporation of both organic and inorganic nanomaterials feasible for the delivery of anti-microbial agents aiding in the fight of identifying possible solutions against the rise of AMR (Tadesse, 2018).

Nanotechnology provides a sound platform for adjusting the physicochemical properties of numerous materials and molecules to generate effective antimicrobial agents (Su, 2018). Beyond the physiological barriers current antibacterials do not have ideal pharmacokinetic and pharmacodynamic profiles (Table 2-1). Homing in on the relationships that exists between nanomaterials and their antibacterial activity is cardinal for achieving future successes using nanotechnology. Specific nanomaterials which are antibacterial in nature complements antibiotics dosing. These are a highly promising combinations and currently gaining large interest as they might overcome current difficulties seen with mainstay antibiotics. In addition, nanomaterials can complement and support traditional antibiotics as a desirable *in vivo* carrier (Nurit, 2015).

Nanotechnology has already showcased that the properties it retains can benefit current oral mainstay dosing regimens. These benefits include better optical and structural properties (Souto, 2020). NPs inherently have good *in-vivo* attributes due to their physically smaller size, surface structure and high surface-volume area as compared to other anti-microbial molecules (Hallan, 2016). Various different materials have previously been utilised during the research phase of combining antibacterial

drugs with NP. Those materials include, metals, lipids and polymers (Pignatello, 2018). Polymers which can be either natural (e.g., gelatin and albumin), synthetic (e.g., polylactides and polyalkylcyanoacrylates), or solid lipids (Solid Lipid Nanoparticle-Based (SLNR) (Nasiruddin, 2017).

Antibiotics have physicochemical properties such as poor aqueous solubility and labile nature with processing and storage (Hajipour, 2012). The use of NPs has been demonstrated as an effective strategy for the delivery of antibiotics. NPs protect the antibiotic from degradation during GIT transit and can improve bioavailability (Wang, 2017). Significant variables are the size and distribution of NPs, surface functionalization, concentration and cellular penetration and permeation through biological barriers. Figure 2-2 presents a schematic of the oral delivery pathways of drug-loaded NPs.

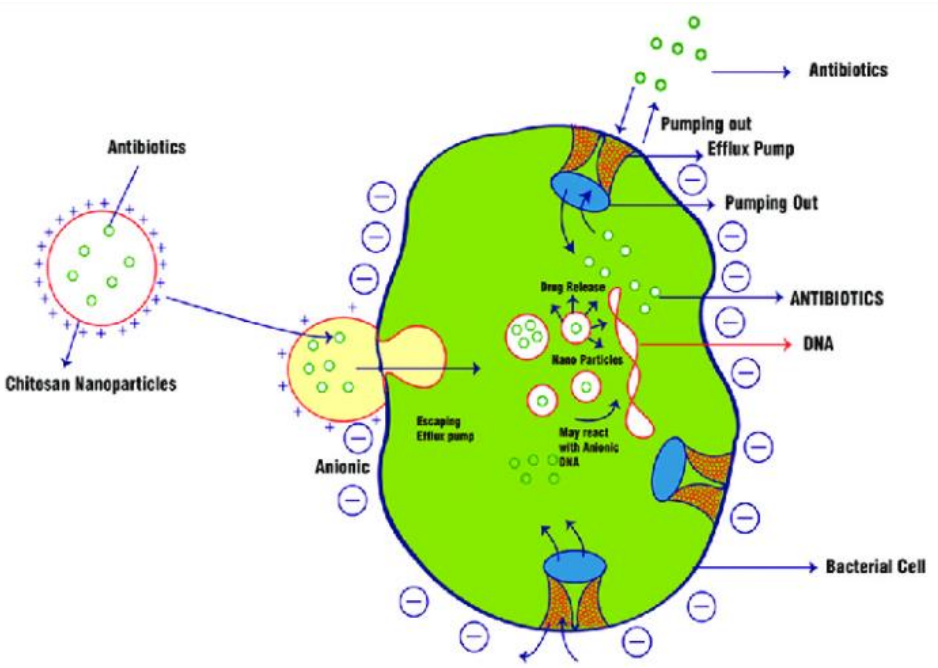

Figure 2-2. Oral delivery routes for drug-loaded nanopolymer and nano lipid structures. An Illustration utilising Chitosan as nanoparticle delivery mechanism (Safhi, 2016). (Permission received for reproduction)

2.4.1 Mechanisms for combating AMR using nanoparticles

Nanoparticles combat microbial resistance through several pathways (Knetsch, 2011). Several types of nanoparticles suppress resistance by adding multiples different pathways to combat microbes simultaneously, including nanoparticles containing chitosan (chitosan NPs), nitrogen oxide-releasing nanoparticles (NO NPs), and metals containing nanoparticles e.g. nanoparticles containing titanium-dioxide (TiO2 NPs), and nanoparticles containing silver (AG NPs) (Al2O3 NPs) (Schairer, 2012).

Nanoparticles have also been used to bypass known pathways of resistance, including intracellular located bacteria, biofilm development, and reduced bacterial cell drug uptake and increased drug efflux (Huang, 2011). Nanoparticles were used to target and deliver antimicrobial drugs to the infection site in order to release higher doses of the antibiotic at the infected site, thus eliminating resistance to the patient with less undesirable drug effects (Friedman, 2013).

2.4.2. Nanoparticles with several synchronized mechanisms of action against microbes

Several kinds of nanoparticles utilizes various different pathways to simultaneously suppress pathogenic microbes. These nanoparticles types as described previously, includes chitosan-containing nanoparticles (chitosan NPs), nitric oxide-releasing nanoparticles (NO NPs) and metal-containing nanoparticles (such as copper, titanium and zinc) (Périchon, 2009).

Multiple gene mutations within the bacterial cell leads to an antibiotic resistant environment. However, nanoparticles make use of various different and effective mechanisms that makes it unlikely for resistance to develop in their presence. Figure 2-3 summarizes and displays the multiple mechanisms of action of NO NPs, chitosan NPs, and several of the different metal-containing nanoparticles as described previously (Blecher, 2011).

2.4.3 Nitric oxide-releasing nanoparticles (NO NPs)

Several simultaneous antimicrobial mechanisms are utililized by nitric oxide-releasing nanoparticles (NO NPs) to make it likely that microbes will develop low resistance to NO NPs. NO mainly exerts its antimicrobial action through reactive intermediates of nitrogen oxide (RNOS), which form after NO reacts with superoxide (O2) (Knetsch, 2011).

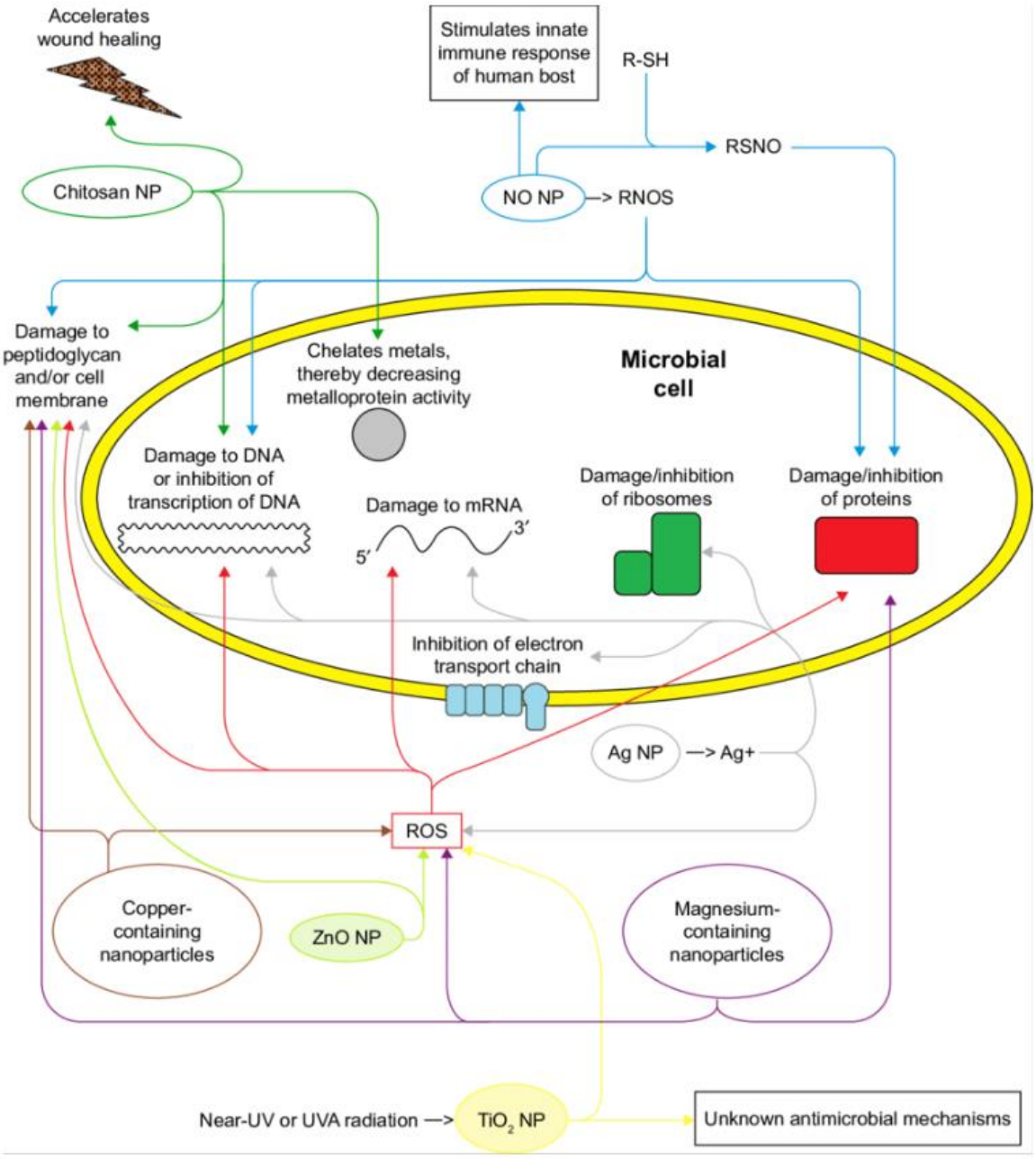

Figure 2-3: Illustration of multiple different mechanisms of antimicrobial action of various nanoparticles (Yang, 2018) (Permission received for reproduction).

Peroxynitrite (OONO), nitrogen dioxide (NO2), and dinitrogen trioxide are included in the RNOS (N2O3). When the NO concentration rises above 1 mM, the formation of such RNOS becomes highly significant through several mechanisms to have antimicrobial activity: 1) RNOS reacts with the amino acid residues of bacterial proteins and also plasma membrane proteins, cys, met, tyr, phe, and trp., 2) RNOS causes DNA direct nitrosative damage, including causing strand DNA breaks, abasic site formation, and cytosine, adenine, and guanine deamination. Additional damage to the microbial DNA is caused by RNOS causing an increased generation of hydrogen peroxide (H2O2) and alkylating agents (Zhang, 2010). RNOS inhibit DNA repair enzymes, including DNA alky transfers, which have S-nitrosylated cystic residues from RNOS, 3) RNOS also reacts with prothesized protein groups, such as Fe–S clusters and haeme. Haeme can be found in enzymes such as nitric oxide synthesis (NOS), CYP450. RNOS irreversibly attach Fe(II) of haeme when at sufficiently high levels, causes removal of haeme from protein and Fe reduction in the bacterial cell, 4) Zinc metalloproteins are also inactivated by RNOS and therefore inhibits microbial cellular breathing, 5) RNOS also triggers peroxidation of lipids (Schairer, 2012).

Finally, the innate immune response in the human host can be stimulated by NO as well. Some bacteria can already express enzymes which protect against nitrosative damage at physiological concentrations of NO in the host in response to NO exposure (Deurenberg, 2009). These enzymes include flavohemoglobin in *K. pneumoniae, S. aureus, E. coli, S. typhimurium*, and *P. aeruginosa*, lactate dehydrogenase in MRSA and MSSA strains of *S. aureus*; and DNA repair enzymes in *S. typhimurium, P. aeruginosa*, and *E. coli*.

While these enzymes protect bacteria from physiological concentrations of NO, they are ineffective at high NO concentrations delivered by NO-releasing nanoparticles, such as NO containing NPs (Blecher, 2009). NO NPs have been seen to significantly inhibit the growth of antibiotic-resistant bacteria, including *E. faecalis, K. pneumonia, E. coli, P. aeruginosa* (Zhang, 2010). Once dosed at a concentrations of 1.25–5 mM, NO NPs combat MRSA, *E. faecalis, E. coli, K. pneumoniae,* and *P. aeruginosa* in culture. Applied topically NO NPs supresses the bacterial growth in infected wounds in mice, intramuscular abscesses and dermal abscesses (Zhang, 2010).

In several *in vitro* and *in vivo* studies, the Hydrogel/glass composite NO NP platform has also had antimicrobial activity against a broad array of drug-resistant bacteria (Friedman, 2008).

Numerous dissimilar antimicrobial drugs could be encapsulated within the same nanoparticle for targeted delivery. The rise in resistance to multiple agents found inside these nanoparticles is impossible, presumably because it would entail multiple simultaneous gene mutations and the deployment of other resistance mechanisms in the same bacterial cell (Lied, 2012). In addition, incorporating multiple different pharmacological agents within the same nanoparticle can result in higher antimicrobial efficacy which is more likely to overcome existing mechanisms of drug resistance in microbes relative to dosing each drug alone (Talluri, 2016).

2.4.4 Nanoparticles that resolves the amplified antibiotics efflux and decreased uptake by bacteria

There are two distinct types of nanoparticles, called liposomes and dendrimers, which can overcome the resistance mechanisms of reduced absorption and increased drug efflux from bacterial cells (Jayaraman, 2009). A liposome is a sphere-shaped vesicle whose cell wall consists of one or more lipid bilayers. Either of these bilayers includes amphipathic lipids that are mostly phosphatidylcholine and usually include cholesterol to increase membrane stiffness (Huang, 2011). ‘‘A liposome with an antimicrobial drug can easily fuse with the microbial cell plasma membrane and then release a high drug level all at once into the microbial plasma membrane or cytoplasm. Therefore, liposomes circumvent the function of tolerance to lower intake of drugs. Faster distribution and increased cytoplasmic amounts of the drug occur in liposomes as well. This drug concentration is sufficiently high to bypass transmembrane pumps, which catalyze the increased drug efflux from the microbial cell (Lied, 2012). Liposomes thus have counteract the mechanism of resistance to increased drug efflux. Lastly, penetrating into bacterial cells, liposomes loaded with an array of multiple antimicrobial drugs allows these different classes of antibiotics greater and quicker antimicrobial activity, destroying these microbes until new mutations evolve that can contribute to resistance to liposome-based nanoparticles.

These mechanisms showed a minimum of 12 times the concentration of oleic acid encapsulated in the liposome (MBC) relative to the free of MRSA oleic acid (Huang, 2011). Moreover, a model MRSA dermal infection, liposome oleic acid, decreased more than 500 times the amount of bacterial cell loads in comparison to empty liposomes and thus eliminated the most of the bacterial cell mass within 48 hours of exposure. Vancomycin also illustrates an improved bactericidal activity against MRSA loaded into liposomes and teicoplanin (an antibiotic semisynthetic glycopopeptide) (Wang, 2017).

2.4.5. Nanoparticles that prevent or overcome biofilm formation

Most nanoparticles can prevent or even resolve the creation of biofilms by various organisms (Hernandez-Delgadillo, 2012). Hetrick (2009) states that NO NPs consisting of silica-killed microbes exist in already formed biofilms like *salmonella, S. aureus*, and *E. coli*. Ag NPs prevent biofilm growth by, for example, inhibiting the production of new bacterial cells on colonizing medical equipment surfaces, such as inhabitating catheters or on existing biofilm surfaces.

2.4.6 Nanoparticles that combat intracellular bacteria

To combat intracellularly located bacteria, nanoparticles have also been used. They are small enough to be phagocyticized by a host immune system. These nanoparticles are adsorbed into the host cell so they unleash a variety of primed drugs against this intracellular disease (Hajipour, 2012). In addition, nanoparticles can release high antimicrobial agent concentrations inside infected host cells while keeping the total quantity of drug administered low compared to conventional dosing (Huh, 2011).

The high local dose in the infection site destroys the intracellular bacteria before resistance develops, the lower total dose reduces the risk of bacteria developing drug resistance beyond nanoparticles action site. In alveolar macrophages, nanoparticles may combat intracellular microbes. Intracellular microbes that intracellularly spread in alveolar macrophages are phagocytized and include *M. Pneumonia, tuberculosis* and *legionella pneumophila* (Hajipour, 2012).

Adhesion of mannose to nanoparticles carrying antimicrobial drugs makes it possible to target alveolar macrophages that strongly express mannose surface receptors. Liposomes carrying second-generation quinolones (such as ciprofloxacin) conjugated with mannose have been administered via the pulmonary route and have been shown to have high selectivity for alveolar macrophages. It has also been shown *in vivo* that mannose-conjugated liposomes contribute to significant higher concentrations of antimicrobial drugs in alveolar macrophages compared to type II pneumocytes (Hernandez-Delgadillo, 2012).

2.5. Advanced Nano-Enabled Drug Delivery Technologies

2.5.1. Achieving a desirable pharmacokinetic profile

Nanoparticles may serve as a medium or distributor for enhanced and defined delivery of drugs to the site of infection. One of several primary goals of using these materials is to increase the bioavailability of drugs while at the same time reducing the amount of active pharmaceutical ingredients in order to reduce toxicity (Fernando, 2018). The host organism often does not tolerate high conventional doses of antimicrobial (oral or parenteral) medications well, whereas the alternatively used lower doses are inefficient and sub-optimal. (Nurit, 2015).

Due to their favourable pharmacokinetic (PK) attributes owned by NPs, utilising this technology to combat the above listed prevalent issues can possibly be surmounted (Siyung, 2019). In this context an ideal PK profile will include (but not limited to): enhanced drug solubility, offer stealth for immune evasion, modulate drug release characteristics, target drug molecules to desired sites of infection and where applicable deliver multiple drugs conjugated or loaded within NPs simultaneously which ultimately leads to an improvement of the therapeutic index and an optimized PK profile (Inzana, 2016). An example of such a treatment regime would be in Tuberculosis where isoniazid and rifampicin are dosed together for six months depending on a patient's clinical workup and diagnosis.

2.5.2. Examples of Advanced oral nano-enabled antimicrobial delivery technologies

Various types of nanocomposite material have been utilised with the aim of increasing the effective dosing parameters of antimicrobial drugs and decreasing the above-mentioned shortcomings.

Inorganic NP such as silver (AgNPs) are well-known antibacterial agents versus a broad spectrum of Gram-positive and Gram-negative bacteria, including antibiotic-resistant bacterial strains. There have been various studies performed to showcase their excellent capacity to act as anti-microbial agents (Díez-Pascual, 2018). Due to various synergistic effects, the combination of AgNPs with other nanomaterials even with antibacterial activity such as graphene oxide (GO) contributes to enhanced antibiotic properties. The 2D layered GO structure can wrap the bacterial cell membrane and induce oxidative stress in the basal plane, thereby damaging the microbe's cell membrane. A similar study done by Buszewski, (2018) illustrated that biosynthesized AgNP by a microorganism *S. durhamensis* had significant anti-bacterial properties.

The conclusive observations from that study suggested that nanoparticles' antibacterial activity is determined by their size, shape, and concentration. Large nanoparticles allow bacterial cells to be contacted by large surface areas, which means that smaller particles may have higher percentages of interactions relative to larger particles.

Nanoparticles of less or equal to 25 nm possess the highest antibacterial activity. Smaller nanoparticles exhibit higher toxicity toward bacterial pathogens, as these nanoparticles likely diffuse more easily relative to those larger in size (Buszewski, 2018). Another nanoantibiotic study set out by Khurana, (2018) tested the use of copper (CNP) substituting silver-nanoparticles (SNP) due to the better economic profile related to copper’s lower cost. Their results illustrated that the biocidal activities of CNPs are better than SNPs. Minimum inhibitory concentration (MIC) values of CNPs are 10 times lower as oppose to those values seen for SNPs.

These improved biocidal activities of CNPs would make it more affordable to reproduce and apply to other more traditional antibiotic agents currently in usage against microbes who are most susceptible to this class of anti-microbial pharmacological action. This notion is supported by the fact that Superbugs are unlikely to develop any form of resistance against inorganic - metal nanostructures as they commonly do against current conventional antibiotics due to the random targeting capabilities of these agents (Khurana, 2018).

Cancer theragnostic have also seen the impact of nanotechnology where Talluri, (2016) postulated that nanoparticles can easily permeate into the leaky vasculature-tumour tissue (where healthy tissue has a uniform vasculature) and can deliver the drug in the controlled manner at the site of tumour tissue.

Due to economical constraints in this early stage of research, nanoantibiotic scientists are adapting their NP formulation techniques (Khurana, 2018). Phytopharmacological NP formulation methods have been applied to attain a non-toxic and environment friendly approaches for the ecologically friendly and sustainable bio-synthesis of NPs with high purity, stability and low polydispersity (PDI). In such a study, *Justicia glauca* (aqueous leaf extract) mediated gold-nanoparticles (AuNPs) synthesised at room temperature, shows an antagonistic effect loaded with Clarithromycin (CLR) and Azithromycin (AZM) antibiotics against various oral pathogenic bacteria and fungi (Emmanuel, 2017). This current technology has also been used in surgical applications, and not only focusing on oral dosing. García-Alvarez, (2017) have used a bioceramic and polyvinyl alcohol (PVA) mixture prepared by rapid prototyping with an external coating of gelatin-glutaraldehyde (Gel-Glu) with three different model antibiotic drugs; levofloxacin, vancomycin and rifampin. Their findings suggests that these hierarchical three dimensional multidrug scaffolds are promising candidates as platforms to be used for local bone infection therapy post operatively.

2.6. Concluding Remarks

Majority of antimicrobial resistance mechanisms which have been researched and developed to date have shown promise in the race against AMR. This is largely due to the pharmacological mechanism of action (MOA) of NPs which is in direct physical contact with the bacterial cell wall and promotes cell death without the need to penetrate the intra-cellular compartments, or when delivering a known anti-bacterial molecule, can offload the drug at the site of infection. This raises the hope that NPs would be less prone to promoting resistance in bacteria than currently used antibiotics as well as attain sufficient clinical benefit (Linlin, 2017).

Being more innovative with utilizing current available drug molecules in a variety of different antimicrobial drug classes conjugated in unique physicochemical manners to a variety of nanoparticulate carrier molecules such as described above, can possibly be a potential avenue which can assist to combat the pressing issue of anti-microbial resistance (Gao, 2018).

The utilization of nanoparticles and nanotechnology in addressing the urgent need for more efficient antimicrobial treatment will be a cardinal step in research identifying a solution for multi-drug resistant microbes.

CHAPTER 3
MATERIALS AND METHODS FOR THE SYNTHESIS OF EUDRAGIT RL-100 AND PLURONIC F127 NANOPARTICLES FOR THE DELIVERY OF AMPICILLIN

3.1 Materials

Pluronic® F-127 (PEP-PPO-PEO) (Mw=12 600 g/mol**)**, Eudragit RL 100 (EU-RL), ampicillin (AMP) anhydrous ($C_{16}H_{19}N_3O_4S$) (Mw=349.40 g/mol) and a dialysis bag (10-12 kDa) were purchased from Sigma-Aldrich (St. Louis, MO, USA**)** to prepare the nanoparticles (NPs)**.**

Tryptone Soya agar (TSA), Tryptone Soya broth (CMO 129B), along with 0.04 mL Iodonitrotetrazolium (INT) dye were used for the *ex vivo* antibiotic activity assays with pathogen utilized *S. aureus* (#25923). All other solvents and reagents were of analytical grade and de-ionized water was used throughout the study.

3.2 Synthesis of the AMP-loaded EU-RL-PF127 nanoparticles

A modified nanoprecipitation method was used to prepare the nanoparticles (NPs) as described by Salatin, (2017). Briefly, 70 mg of AMP was dissolved in 4 mL de-ionized water. A total of 700 mg of EU-RL was then dissolved in 10 mL of acetone. Both solutions were stirred using a magnetic stirrer for 20 minutes. The aqueous AMP solution was then added dropwise over a time period of 1 minute into the organic EU-RL solution and stirred for 30 minutes using a magnetic stirrer to ensure complete incorporation of AMP within the polymer framework.

Separately, 400 mg of PF127 was dissolved in 20 mL de-ionized water and magnetically stirred for 20 minutes. The AMP-EU-RL solution was then introduced dropwise into the PF127 and left stirring overnight (24 hours) to ensure complete chemical incorporation of the polymeric solutions and evaporation of any excess organic solvent under a fume hood. A 5 % (w/v) mannitol solution was then added as a cryoprotectant and stored at -80 °C for 24 hours before lyophilization.

A lyophilizer (FreeZone® 2.5, Labconco®, Kansas City, MS, USA) was used to produce a stable free-flowing powder of the NPs. Post-lyophilization the NPs were placed in plastic agar plates under parafilm and stored between 18 – 22 °C in a dry cabinet. A same synthesis procedure was followed to prepare AMP-free NPs.

3.3 Evaluation of the chemical structure integrity of the AMP-loaded EU-RL-PF127 nanoparticles

Overall vibrational spectroscopy investigations were undertaken on the synthesized AMP-loaded NPs, native AMP and AMP-free NPs to evaluate and map the stability of any chemical structure modifications that occurred as a result of blending EU-RL and PF127 as well as NP formation. FTIR analysis was undertaken using a Perkin Elmer Spectra 2000 Vibrational Spectrometer with a MIRTGS Sensor (PerkinElmer spectroscopy 100, Lantrisant,Wales, UK) equipped with a diamond gemstone interior indicator component. Analysis was undertaken between 650 and 4000 cm^{-1} wavenumber series with a 4 cm^{-1} resolution and 64 scans per spectrum.

3.4 Determination of nanoparticle size and stability

The mean particle size**,** zeta-potential and polydispersity index (PdI) were determined by initial dispersion of 2mg samples of NPs in deionized water. Results were acquired by active dynamic beam scattering (DLS) on a Zetasizer Nano a ZS instrument (Malvern Instruments, Worcestershire, UK). The particle size was calculated as a z-average size (± SD) and size distribution was determined by the polydispersity index (PDI). Membrane filters of 0.22 µm where used to ensure sample purity. Each sample was measured in triplicate (N=3). Results were expressed as a mean.

3.5 Morphological analysis of the nanoparticles

The morphology of the NPs was evaluated using a JEOL 840 SEM (JEOL, Japan) under various magnifications at 20 keV.

Samples of NPs were prepared with carbon and argon high pressured air. Micrographs were obtained and qualitatively evaluated for the surface morphology of the samples.

3.6 Thermoanalytical characterization of the nanoparticles

Thermoanalytical and thermophysical testing of the AMP-loaded NPs was undertaken. Samples of native and AMP-loaded NPs were analyzed to determine phase transitions as well as thermally induced chemical reactions and decompositions by Differential Scanning Calorimetry (DSC). Data was recorded using a Mettler Toledo DSC-1 STARe system, heated from 25-300 °C, at a heating rate of 10 °C per minute resulting in thermograms of heat flow versus sample temperature.

3.7 Homo- and hetero-aggregation characterization and stability testing of the AMP-loaded nanoparticles

The physical stability of the NPs was characterized using optical interaction analysis using a Turbiscan™ LAB (Formulaction, L'Union, France) instrument. A 20 mL aliquot of AMP-loaded and AMP-free NPs were analyzed for physical stability over a period of 1 hour. Samples of NPs were suspended in de-ionized water and introduced into specialized sample holders and analyzed at predetermined intervals over a period of 5 minutes at 25 ± 0.5 °C. ''The instrument was fixed with a pulsed near infrared light source moving vertically along the sample collecting data at 40 µm intervals. A 180° positioned transmission detector detected transmitted light whereas a backscattering detector, positioned at 45°, detected rebounded light in response to the light-scattering effect by the suspended NPs.'' The changes in backscatter (ΔBS) measurements were used to assess the physical stability of the nanosystem.

3.8 Determination of the AMP-loading efficiency within the nanoparticles

The drug entrapment efficiency (DEE%) (Equation 1) was calculated for the nanoparticles by directly dissolving a known mass of NPs (25 mg) in 5 mL of acetone and centrifuged at 4000 rpm for 10 minutes.

The amount of entrapped drug was measured by UV-visible spectrophotometry at a detection wavelength of 270 nm. A typical standard curve (R^2 = 0.9787) (Figure 3-1) was used to determine the loading of AMP into the NPs and the DEE% value was computed using Equation 1.

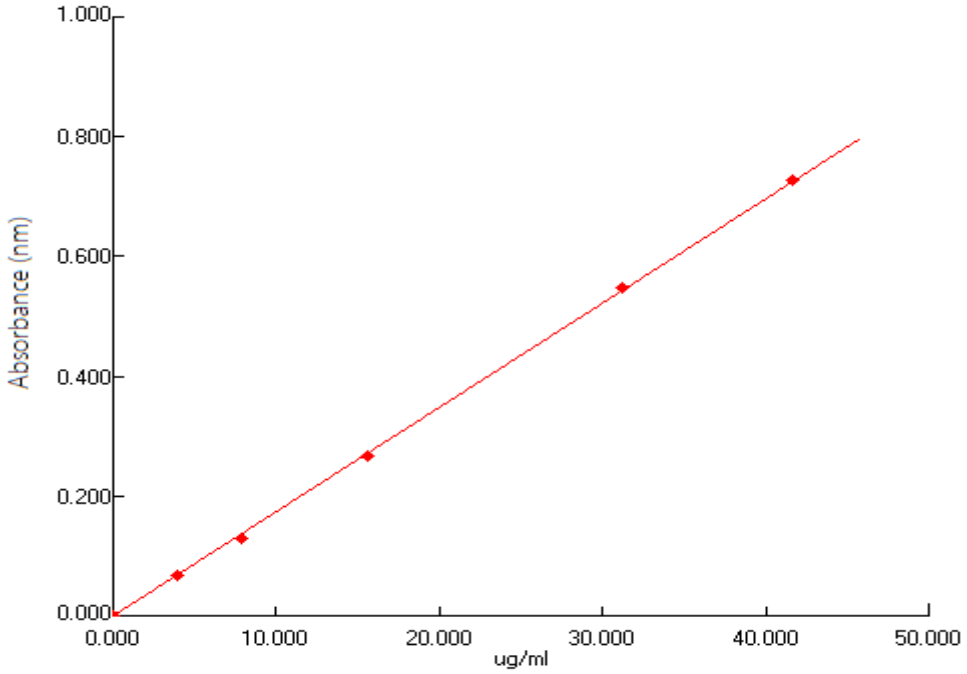

Figure 3-1: Calibration curve showing the relationship between ampicillin concentration in PBS and absorbance.

$$DEE\ (\%) = \frac{Mass\ of\ AMP\ in\ EU{-}RL{-}PF127\ nanoparticles}{Mass\ of\ EU{-}RL{-}PF127\ nanoparticles}\ x\ 100 \quad (1)$$

$$AMP\ loading\ \left(\%\frac{w}{v}\right) = \frac{Mass\ of\ AMP\ in\ U{-}RL{-}PF127\ nanoparticles}{Mass\ of\ nanoparticle\ yield}\ x\ 100 \quad (2)$$

3.9 *In vitro* release studies of AMP from the nanoparticles

In vitro release of AMP from the NPs was determined in simulated gastric fluid (SGF) (PBS pH 1.2; 37 ^{0}C) as well as in simulated intestinal fluid (SIF) (PBS; pH 6.8; 37 ^{0}C) for a duration of 2.5 hours and 24 hours, respectively. AMP-loaded NPs (25 mg) were introduced into dialysis tubing and immersed into 80 mL of release medium in an

orbital shaking incubator (LM-530-2, MRC Lab Instruments Ltd., Hahistadrut, Holon, Israel) set at 25 rpm at 37 ^{0}C.

At predetermined time intervals 3 mL samples were withdrawn in order to determine AMP concentration by UV spectroscopy at 270 nm and 3 mL of drug-free release medium was replaced to preserve sink conditions. This approach was sufficiently sensitive for investigating drug release from the NPs with release intervals of >1 hour. *In vitro* release studies of AMP-loaded NPs enclosed in gelatin capsules was also undertaken.

3.10 Bioassay of antibacterial activity

The pharmacological efficacy of the nanosystem was measured by a simple disk diffusion method and ~~a~~ the more quantitative Minimum Inhibitory Concentration (MIC) analysis against *Staphylococcus aureus* (ATCC#25923). The conventional oral formulation (AMP anhydrous in powdered form) and the AMP-loaded EU-RL-PF127 nanosystem were tested. The AMP-free NPs also underwent the same testing procedure for comparative pharmacological efficacy assessment. AMP anhydrous was used as drug control. Samples of NPs were dissolved in distilled water and diluted accordingly throughout the 96 well plate to detect the MIC value. Nanoparticle samples of 1 mg and 10 mg were used to in both bioassay studies against their blank counterparts.

3.10.1 Agar Disc Diffusion Studies

Basic agar disc diffusion studies were conducted as preliminary qualitative assays to screen the antimicrobial activity of loaded nanoparticles. 20 mL of tryptone Soya agar (TSA) plates were inoculated with 100 μL standardised inoculum of the test microorganism *S.aureus* (#25923). A disc with a diameter of 6 mm was placed aseptically with 1 mL volume of the drug loaded nanoparticles with antimicrobial agent at desired concentrations (1 mg and 10 mg) were introduced into their separate plates. Agar plates were incubated for 24 hr at 37 °C. Iodonitrotetrazolium chloride (INT) indicator dye (0.04 mg/mL) solution was sprayed onto inoculated discs to visualise the inhibition zones.

3.10.2 Minimum Inhibitory Concentration (MIC) Assay

This MIC microdilution bioassay was used to quantitatively assess the level of antimicrobial activity of the studied nanosystem. A method was used with Tryptone Soya broth (TSB) in a 96 well plate with an eight-time diluted sample from A -> H. Aseptically, 100 μL of distilled water was added to each well, followed by a 100 μL of dissolution samples (3 columns of actively loaded NPs and 3 columns of blank NPs) (diluted 1 : 10 with sterile water) which were added to the first six rows of the microtitre plates. Doubling serial dilutions were performed. Microtitre plates were sealed with an adhesive film to prevent the loss of any volatile samples and incubated for 24 hours at 37 °C. Inhibitory concentration determinations were visually observed with an INT dye of 0.04 mL after 4 hours of introduction. Acetone was utilised as negative control and AMP as positive control during these experiments. Culture control was *Staphylococcus aureus* (ATCC#25923).

3.11 Statistical Analysis

Data for the preparation and characterization of nanoparticles, drug release and bioassay studies were processed and analysed by basic Origin software (version 8.5.0 SR1, Origin Lab corporation, Northampton, MA, USA). Descriptive statistics where used throughout this study. All measurements were performed in triplicate (N=3) and presented by the mean, ± standard error of the three experiments throughout this report.

3.12 Concluding remarks

Various different categorization laboratory techniques were utilized to study the nanoparticles (NPs) (both loaded and blank), produced by a modified nanoprecipitation method as described by Salatin, (2017). These undertaken studies were to evaluate the numerous physicochemical, *in vitro* pharmacokinetic and morphological properties of the developed delivery system.

The evaluation of the chemical structure integrity and stability of both nanoparticle formulations are discussed in the following chapter with in depth analysis of the characterization studies undertaken. These will assist in drawing conclusions to the possibly validity of this synthesis method. Additional *in vitro* release studies discussed in the following chapter will provide further insight with regard to the kinetic order of the drug lease of the loaded nanosystem. Determination of drug release in two different simulated gastric mediums, and antibacterial activity via two standard bioassays assessed the inhibition concentration of drug loaded nanoparticles of a standard pathogenic inoculum agent.

CHAPTER 4
RESULTS AND DISCUSSION OF THE SYNTHESIS OF EUDRAGIT RL-100 AND PLURONIC F127 NANOPARTICLES FOR THE ORAL DELIVERY OF AMPICILLIN

4.1 Introduction

There are numerous drawbacks in the oral dosing of antibiotics that lead to poor bioavailability and eventually to drug resistance (Oledzka, 2014). Oral antibiotics typically pass through the intestinal wall and the liver, which contain numerous inactivating enzymes and undergo first-pass metabolism, and this means that only a fraction of oral antibiotics eventually enter systemic circulation and low concentrations reaches the targeted sites (Hetal, 2010). The use of nanotechnology can alleviate both the burden to the patient and the healthcare system by affording a more targeted approach to treating protracted infections at the site as opposed to the current non-specific systemic approach (Oledzka, 2014). Polymer nanoparticles (NPs) are constructs that are capable of mechanically enclosing drug molecules within them and maintain their pharmaceutically stable structure to ensure the effective distribution of drugs to a particular intracellular compartment (Tao, 2019). This approach also increases the drug bioavailability by stabilizing drug molecules within nanoparticle dispersion systems such as nanomicelles, nanoparticles, nanocrystals, nano-emulsions or nanoliposomes (Tao, 2019).

Ampicillin (AMP) is a β-lactam antibiotic with a broad spectrum of antibacterial activity against Gram-positive, Gram-negative and anaerobic bacteria (Rafailidis, 2007). The therapeutic dose of AMP ranges between 1.5-12 g/day for adults (depending on clinical manifestations) and 150 mg/kg/day for children. After administration the maximum plasma concentration (C_{max}) depends mainly on the patient's age due to renal function (Meyers, 1993). There are other physiological factors that also play a role on how AMP is degraded after oral administration (Meyers, 1993). Dafnomilis,

(2019) mentioned that AMP is a frequently utilized and widely available antibiotic that appears on the essential drug list of the world health organization (WHO).

In addition, many previous studies were undertaken to improve the oral bioavailability of AMP and provide more targeted drug release but many were challenged by the limitations posed with drug targeting in the gastrointestinal track (GIT) and at the site of action. Previous studies have used microspheres with ethylcellulose and poly(ε-caprolactone) matrix and have shown favourable AMP release kinetics (Abdelmalek, 2014). It was postulated that the sustained release was largely due the presence of specific functional groups within the matrix that favourably interacted with the anionic carboxylate group of AMP and its interaction with the cell membrane (Abdelmalek, 2014).

Herein this study the aim is to fabricate a pharmaceutically stable nanosystem utilizing a blend of Eudragit RL-100 (EU-RL) and Pluronic F127 (PF127) as the polymeric framework. EU-RL is a cationic polymer that can impart mucoadhesive properties by increasing the interaction between mucin and NPs in the GIT and thereby increase the AMP absorption and bioavailability after oral administration (Jiao, 2002). PF127 is a synthetic thermo-responsive tri-block co-polymer (PEO-PPO-PEO) that has been widely used for drug delivery applications since it can form *in situ* gel-like structures at body temperature. This feature is desirable to ensure synergistic interaction with the EU-RL to increase the contact time with the GIT membrane for enhanced AMP absorption. Furthermore, the chemical flexibility of PF127 can facilitate functionalization as a future strategy to obtain actively targeted drug delivery using this nanosystem. The AMP-loaded EU-RL-PF127 nanosystem will be characterized for its physicochemical properties to assess its molecular composition and chemical stability using Differential Scanning Calorimetry (DSC), Fourier Transform Infrared (FTIR) spectroscopy and Thermogravimetric Analysis (TGA). Entrapping AMP within a EU-RL polymer framework could potentially enhance the drug release profile, increase the GIT membrane contact time for absorption and improve the oral bioavailability and antimicrobial efficacy of the antibiotic.

4.2 Results and Discussion

4.2.1 Morphological characterization of the AMP-loaded nanoparticles synthesized by nanoprecipitation method.

Anhydrous AMP is slightly soluble in aqueous solution (0.605mg/mL). Due to the low solubility it was vigorously stirred to dissolve resulting in a homogenous solution. This was important as the drug's low water solubility as well as being homogenously distributed assisted in ensuring that a higher amount of AMP was entrapped within the NPs. The nanoprecipitation method is regularly used (Oledzka, 2014) to fixate water soluble drugs in lipid-based polymers to enhance its physiological activity by rendering it more lipophilic for gastrointestinal (GIT) absorption. The nanoprecipitate was formed between AMP and the polymethacrylate-based copolymer (EU-RL) with the addition of a surfactant coating, PF127. Figure 4-1 reveals an SEM image of the synthesized AMP-loaded EU-RL-PF127 NPs. The particle size established with SEM images, shows spherical shaped particles with a narrow size distribution and particle size less than 100nm.

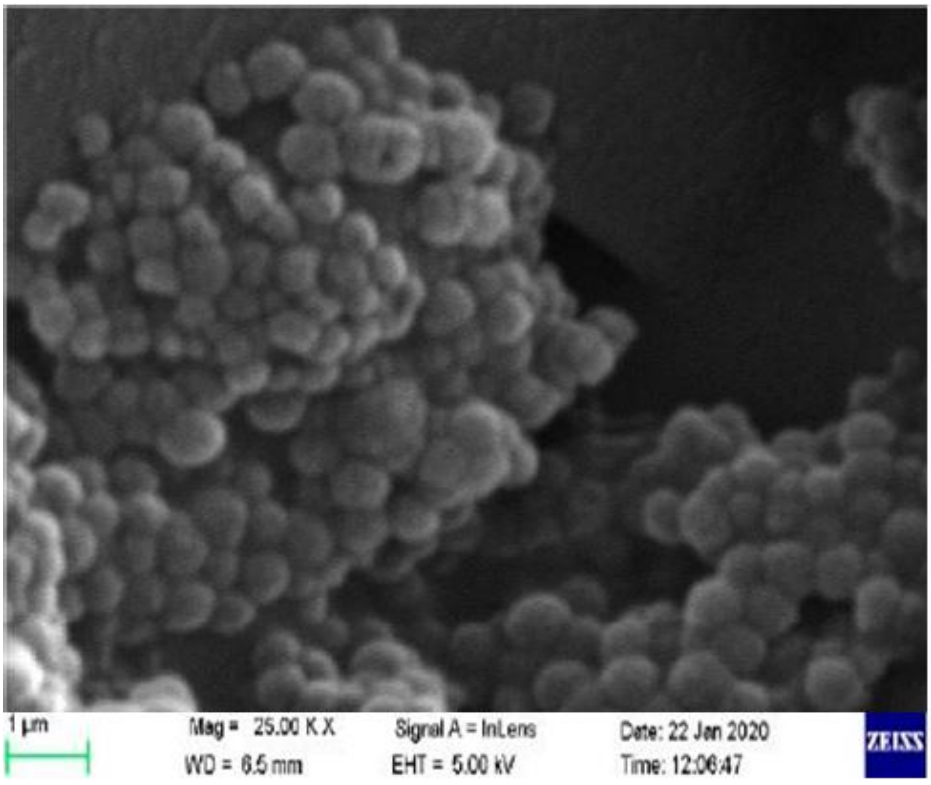

Figure 4-1: Visualization of the AMP-loaded EU-RL-PF127 nanostructure using SEM.

Polymeric NPs are typically spherical, with diameters ranging from 1000 to 10 nm (Freyre-Fonseca, 2016). The AMP-loaded EU-RL-PF127 nanostructure falls well within this range, as well as visually and quantitatively conforming to what is broadly accepted within the nanotechnology industry.

4.2.2. Chemical structural analysis employing FTIR on the copolymeric nanoparticulate formulation

FTIR analysis was undertaken on each polymer, pure loaded drug compound, as well as the drug loaded copolymer formulation. As seen in Figure 4-2, ampicillin displayed peaks at 1689cm^{-1} and 1769cm^{-1}, confirming the presence of the stretching absorbance, reflected by ampicillin, indicative of the beta-lactam ring of the antibiotic (Nairi, 2017). C=O and its amide bonds, was clearly identified in Figure 5a, as well as in the polymeric loaded formulation, indicative of the stability of the beta-lactam ring, once loaded in the nanoparticles (Rozas, 2010). Eudragit displayed a spectra of several characteristic bands at 1702 cm^{-1}, attributed to C=O carboxylic acid groups vibrations, as well as esterified carboxyl groups vibrations, 1152 cm^{-1}, and 1252 cm^{-1} (ester vibrations), 1388 cm^{-1}, 1438 cm^{-1} and 2953 cm^{-1} (CH_X vibrations) and 3225 cm^{-1} (OH groups vibrations) (Hao, 2013).

Pluronic® F-127 displayed characteristic absorption bands at 2878cm^{-1} (-OH) and 1965cm^{-1} (C-O), correlating to its structure (Cerqueira, 2017). The drug loaded copolymer displayed C=O stretching absorption band in the region of 1764 cm^{-1} and O-H stretch in the region of 3452 cm^{-1}. These bands indicate no interaction between the drug and the copolymer, once drug had been loaded.

Pluronic® F-127 displayed an overlap of C=O stretching in the region of 1730 cm^{-1}, as well as stretching vibrations of CH of the PEO unit in PF127 evident in the region of 2880 cm^{-1}. C-O-C stretching was clearly observed in the region of 1099cm^{-1}, also displayed in the copolymer drug loaded formulation. Functional group -OH stretching at wavelengths 3185cm^{-1} and 2935cm^{-1}, was also displayed in pluronic and the copolymer formulation, confirming no chemical interaction besides polymer blending, similar to chemical shifts in the lower wavelength regions of 650 – 1500cm^{-1}, due to -C-H stretching. functional groups illustrating familiar chemical bonds.

The solubility of the loaded drug could be advanced for oral application, due to the amphiphilic nature of Pluronic® F-127. FTIR further displayed a common presence of the beta lactam ring in the drug loaded copolymer, confirming the presence of drug loading in the copolymeric formulation.

The C=O group in Eudrgit, further assists in protecting the loaded drug from degradation in gastric pH conditions. Thus, once passing through the intestinal pH, the nanoparticles will begin to release the loaded drug, for absorption (Kamaly, 2016). The presence of Pluronic®, will also assist in forming a gel formulation, in the presence of intestinal pH, attributing to the release of drug from the nanoparticle formulation. Furthermore, Eudrgit composed co-polymeric nanoparticles have great benefit of mucoadhesive effect. Eudragit is preferred to prepare mucoadhesive nanoparticles as a positively charged polymer as it improves the interaction between mucin and nanoparticles, thereby increasing the bioavailability of drugs (Chaves, 2018).

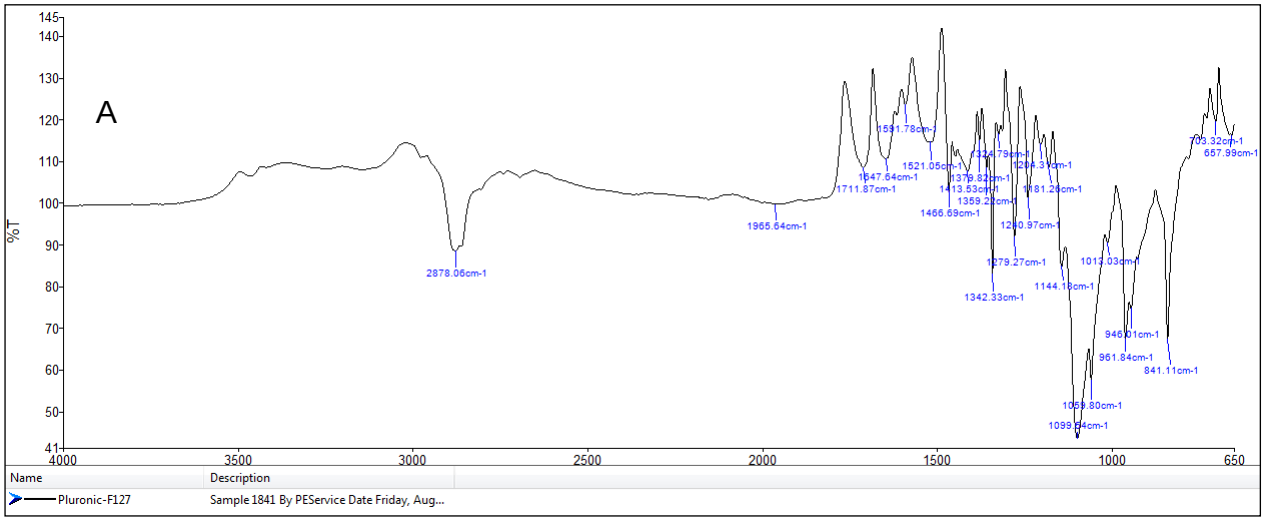

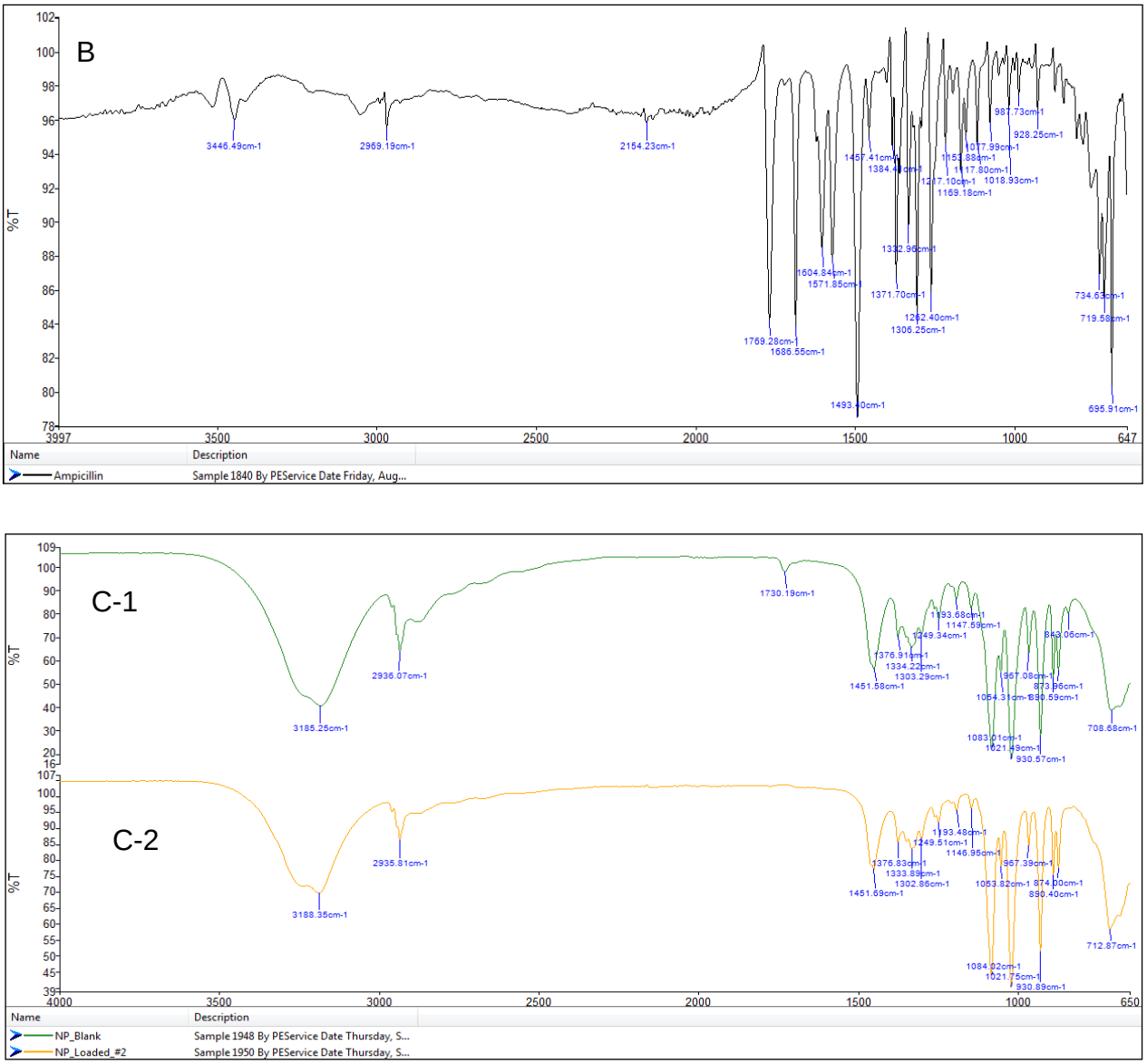

Figure 4-2. FTIR Results. A) Pluronic® F-127, B) Ampicillin Free drug C) Distinction shown between the two NP (blank C-1 and Loaded C-2).

4.2.3 Evaluation of nanoparticle size and stability

Blank nanoparticles and AMP loaded nanoparticles were evaluated for particle size and zeta potential employing the Zetasizer NanoZS analyser (Malvern Instruments Ltd. UK). The particle size difference between the blank and AMP-loaded NPs was minimal as supported by a previous study by Salatin (2016). The blank NPs were found to be slightly smaller in size (69.28 nm ± 0.9 nm) compared to with the AMP

loaded NPs (75.06 nm ± 1.4 nm), suggesting that AMP entrapment was successful with minimal surface adsorbed drug.

The polydispersity index (PDI) of blank and AMP loaded nanoparticles was 0.263 ± 0.09 and 0.445 ± 0.18, respectively. A PDI value of less than 0.5 indicates good and narrow size distribution that is, perfectly uniform/homogenous sample dispersion and stability with respect to the particle size. The same trend was observed during the morphological analysis using SEM. The synthesized NPs (blank and loaded) had an average particle size of 69.28 nm (± 0.9 nm) and 75.06 nm (± 1.4 nm), respectively (Figure 4-3).

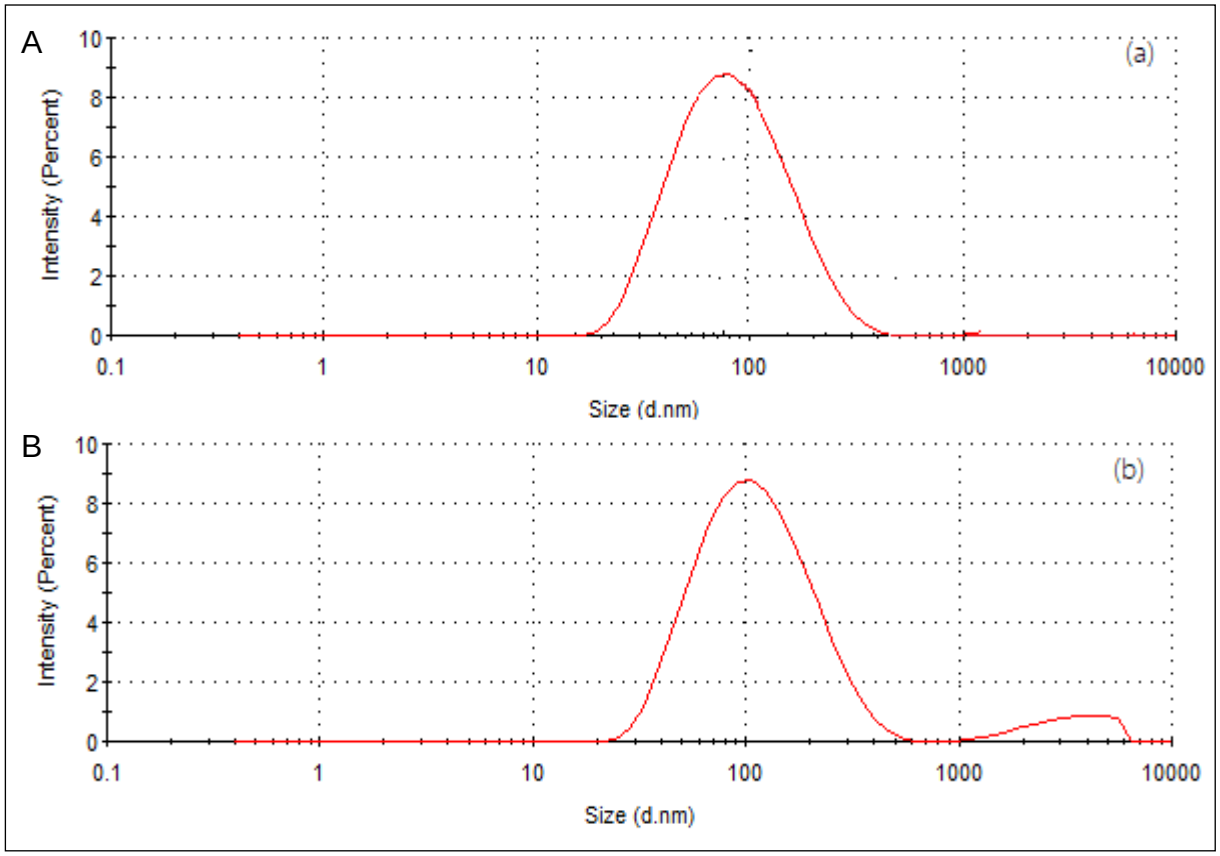

Figure 4-3: Typical particle size distribution to establish the mean particle size of A) Blank NPs and B) AMP-loaded NPs.

The polydispersity index (PDI) and zeta potential values are to be found in Appendix A, table 4-1 on page 73. Due to the uniformity of the peaks visualized during the size distribution, it was concluded that the sample and molecule distribution was uniform. Universally, PDI values of <0.3 are ideal (Maguire, 2018) and reveals a narrow size distribution which is considered acceptable for NPs (Lieleg, 2010).

Phospholipids, poloxamers, and polymers are the main components of polymeric NPs and, once present in formulations, are capable of influencing the zeta potential (Dazon, 2019). The value obtained from the blank-AMP NPs also fell close to this value (0.263 ± 0.09), thereby increasing the validity of the NPs formed using the adopted method. The addition of AMP increased the PDI of the AMP-loaded NPs to 0.445 (± 0.18).

The studied nanostructure for this research (AMP-loaded EU-RL-PF127) contained a surfactant coating - Pluronic® F-127 also known as poloxamer 407. This would have influenced the electrostatic charges of the sample, and close attention was paid to ensure that the correct amount of surfactant was utilized to ensure sample stability. Also important to consider is drug composition and charge, both of which added to sample stability. A relatively high zeta potential value, considered as |± 30 mV|, is important for good physicochemical stability of the colloidal suspension, as large repulsive forces tend to prevent aggregation due to occasional collisions with adjacent nanoparticles (Zielinska, 2020). Furthermore, a colloidal suspension is as such, highly dependent on the electrostatic charges within the sample. This influences the stability of the sample that is ultimately to be dosed. According to another source, Khoshnevisan (2015) a largely positive (> +25 mV) or negative (< -25 mV) zeta potential signifies superior dispersion and sample stability for storage. The blank nanoparticles produced an average zeta potential of -23.3 mV (± 2.7 mV). This is not as high as quoted by Zielinska, but more closer to Khoshnevisan findings. This value indicates adequate dispersion during the sample. The higher negative zeta potential values indicated that the AMP-free NPs were typically more stable compared to the AMP-loaded NPs (-0.319 mV (± 0.7 mV)) from a reactivity perspective. It was determined that at a slightly basic acidity, drug-AMP is anionic (Nairi, 2017) which ultimately had an impact on the stability of the loaded NP making it more reactive and less stable compared to the blank NP.

Additional alterations can be made to the current NPs to influence it's stability and utlimaterly the Zeta potential by introducing other surfactants or other coatings onto the NPs surface, such as poly-ethylene-glicol (PEG) of varying molecular weights (Doktorovova, 2014).

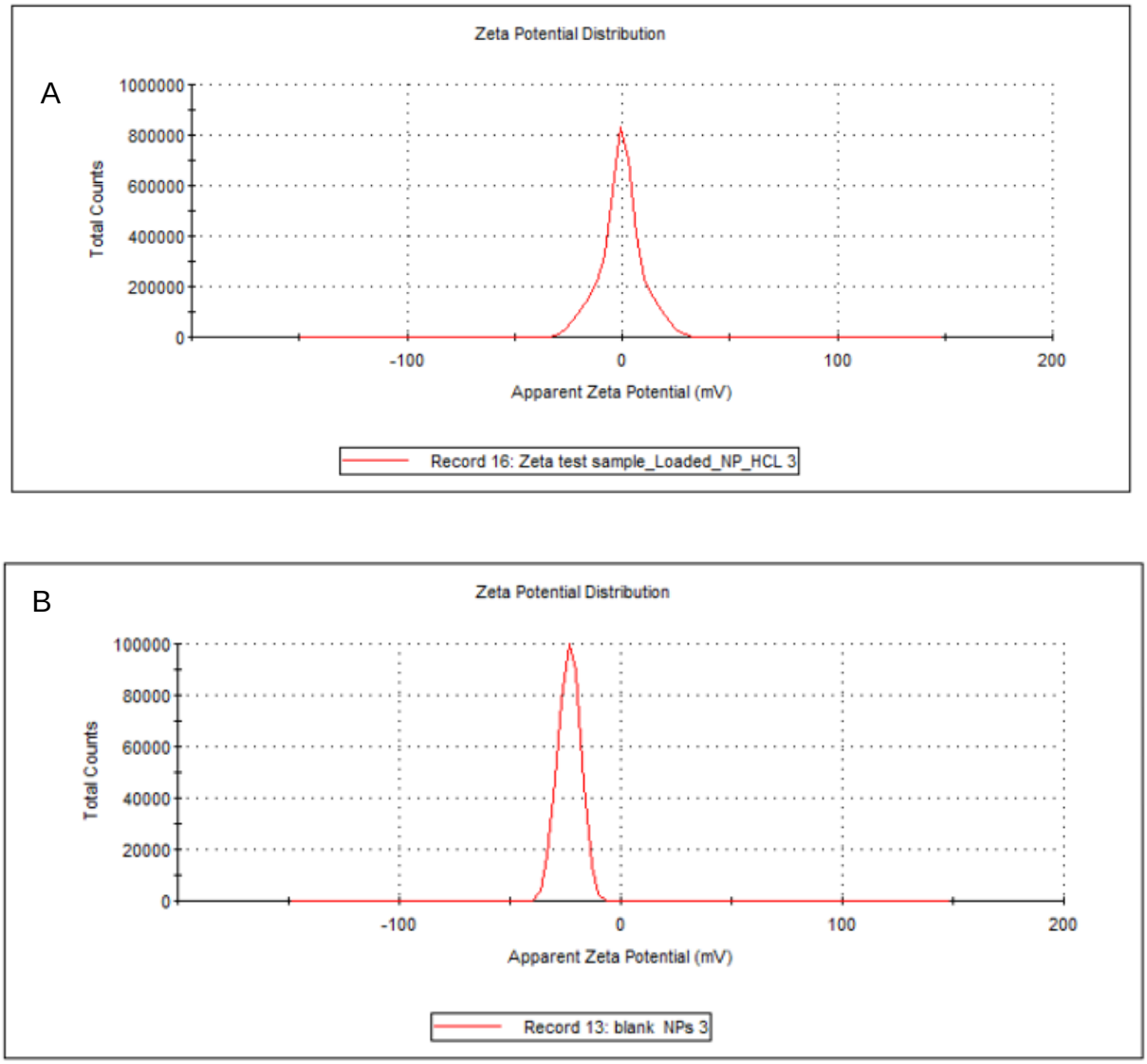

Figure 4-4. Zeta potential profiles of A) AMP-loaded NPs with a value of -0.319 ± 0.7 mV and B) blank NPs with a value of -23.3 mV ± 2.7.

4.2.4 Thermal Analysis of Nanoparticles utilizing Differential Scanning Calorimetry (DSC) the AMP-loaded Eudrigit RL100 – Pluronic® F127 nanoparticles

Heat flow curves (DSC curves) depicted in Figure 4-5 A to 4-5 C for thermal characterisation of AMP-loaded Eudrigit RL100 – Pluronic® F127 nanoparticles showed big endothermic peaks. Identifiable differences in melting temperatures of transitions were obtained. DSC thermogram of Eudrigit RL100 – Pluronic® F127 nanoparticles (Blank) showed a sharp endothermic peak, the melting point at temperature between 160-170 °C, as shown in Figure 4-5 ~~A~~B. AMP-loaded Eudrigit RL100 – Pluronic® F127 nanoparticles also showed two sharp endothermic peaks, one slight peak between 150-160 °C while the other strong peak at 160-170 °C, the AMP melting temperature peak shift was noted and it was possible due to the crystallization temperature effect of the Eudrigit RL100 – Pluronic® F127 copolymer (blank) as shown in Figure 4-5 B. In the DSC thermogram of AMP, a broad endothermic peak is visible at 130-150 °C,as shown in Figure 4-5 A (Yildiz, 2009).

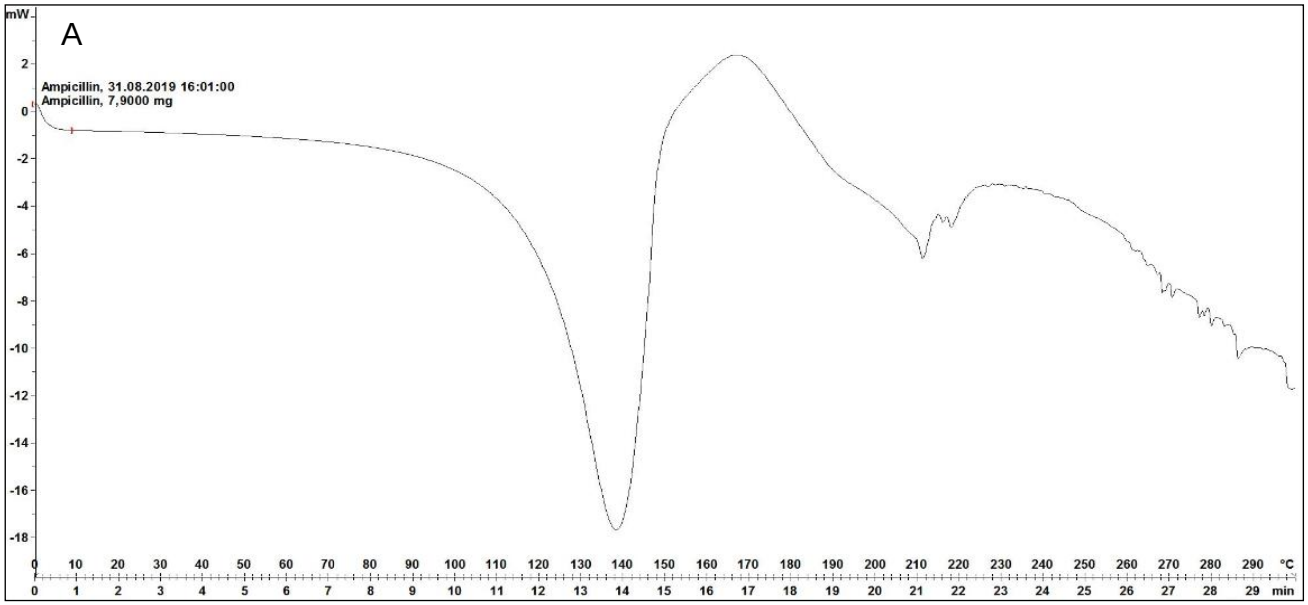

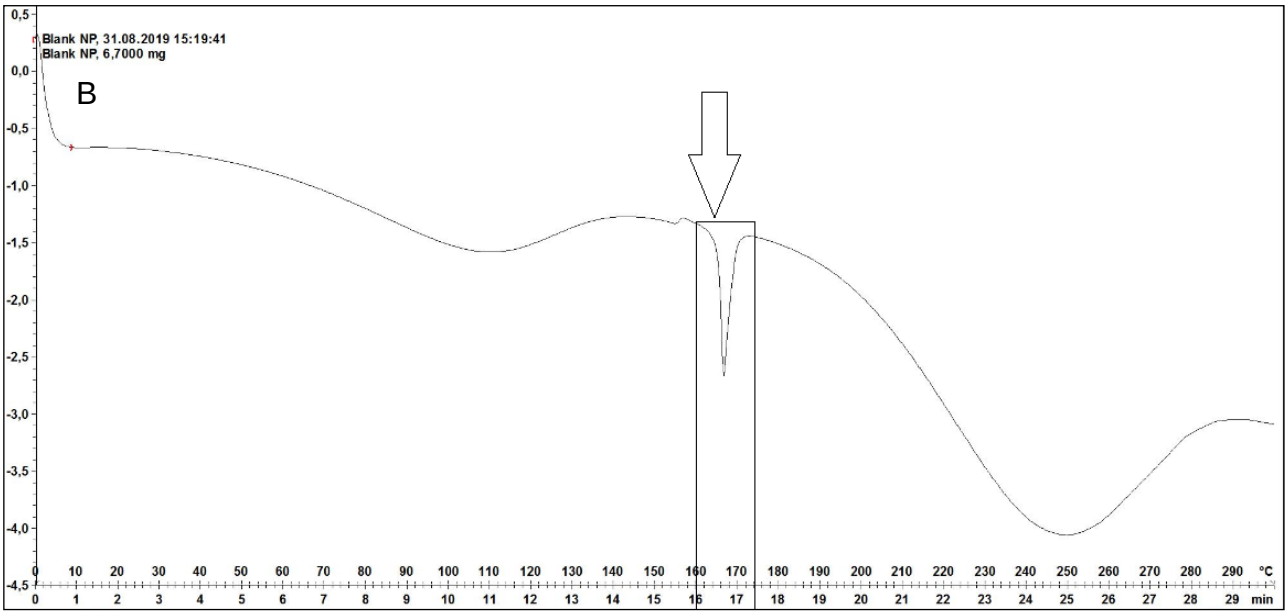

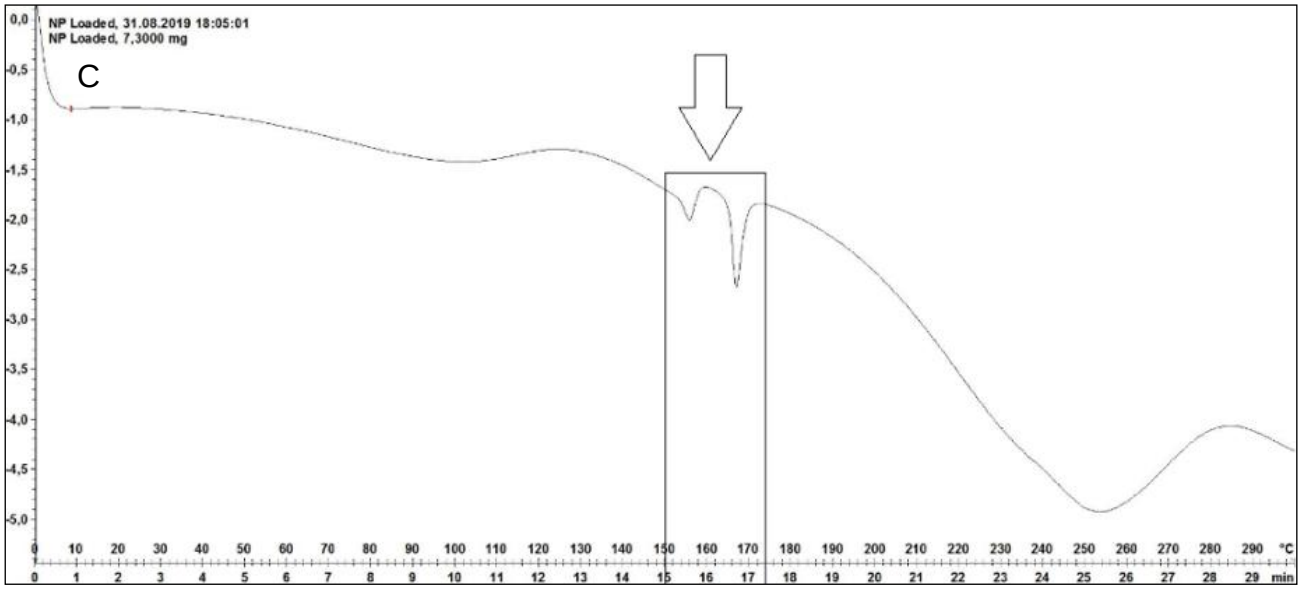

Figure 4-5: DSC curves of AMP (A). Eudrigit RL100 – Pluronic® F-127 nanoparticles (Blank) (B) and AMP-loaded Eudrigit RL100 – Pluronic® F-127 nanoparticles (C)

EU-RL-PF127 NPs assisted with delaying drug crystallization from its previous onset temperature point ± 80 – 90 °C (Figure 4-5 A) to ± 120 – 130 °C (indicated on Figure 4-5 C). This is largely due to the polymer utilized (Eudragit RL 100) which exists in a completely amorphous form with a glass transition temperature (Tg) of about 60 °C (Csóka, 2007). The thermal behaviour of the loaded freeze dried nanoparticles suggested that the polymer inhibited the onset of melting of the drug sooner, increasing stability. This observation is also substantiated from the effect of adsorbed surfactant (Pluronic® F-127) onto the drug loaded nanoparticles, and is in correlation to other similar literature published (Mandal, 2010).

4.2.5 Assessment of the homo- and hetero-aggregation and physical stability of the AMP-loaded nanoparticles

Light scattering analysis (Turbiscan, Formulaction SA, L' Union, France) of the synthesized blank and AMP-loaded NPs was undertaken. Coalescence and flocculation of the NPs were detected through increases in sample particle size. The migration of the NPs was measured in three ways: 1) Sedimentation, 2) Creaming, and 3) Flocculation/Coalescence (Hörter, 1997).

Ultimately, samples were described as either of creaming or sedimentation kinetics. The physical stability of the AMP-loaded and blank NPs were evaluated as a function of intensity of the delta backscattering (ΔBS). Results revealed that AMP-loaded NPs recorded values >40% and 50% for the blank NPs. All samples also had significant variation between 20-35mm where additional transmittance was observed as early on as 2-5mm for native AMP (Figure 4-6 C) indicative of sedimentation kinetics. (Sumaila, 2019).

A

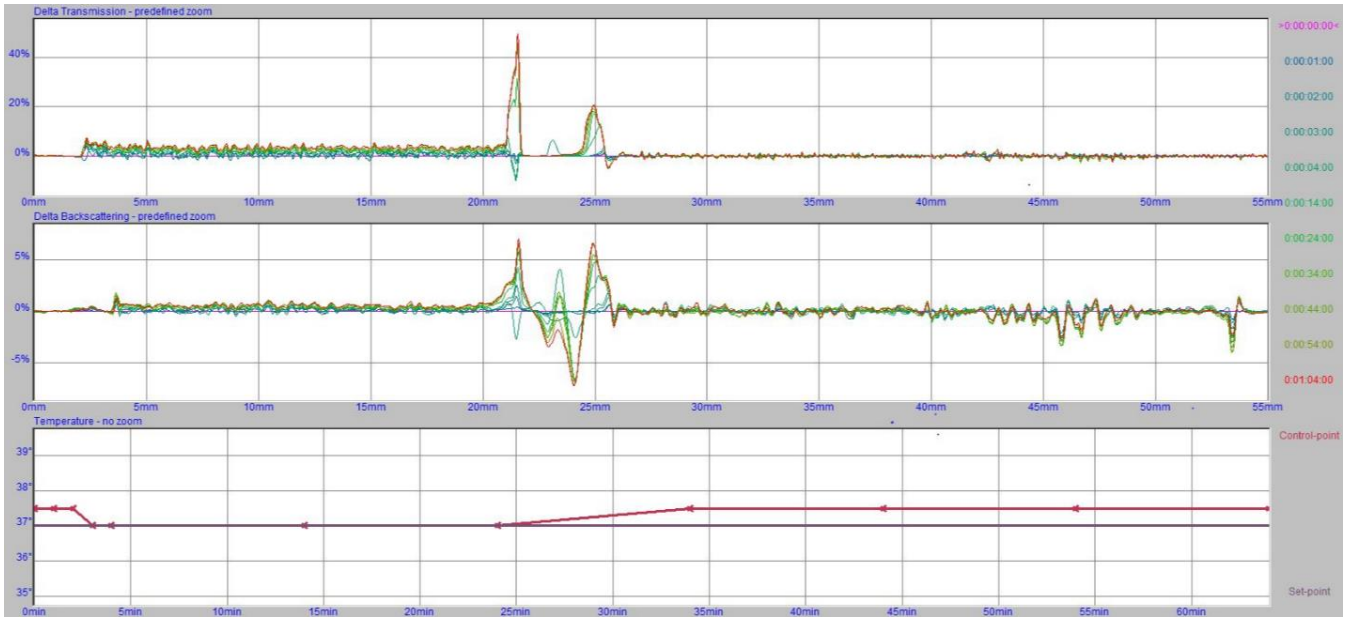

B

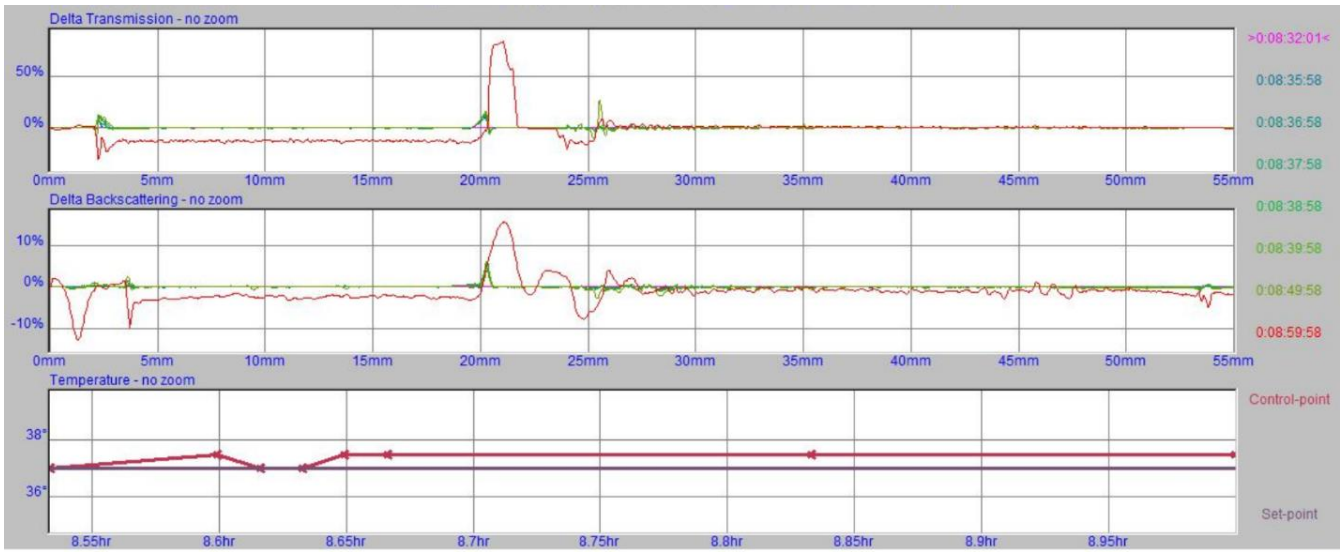

C

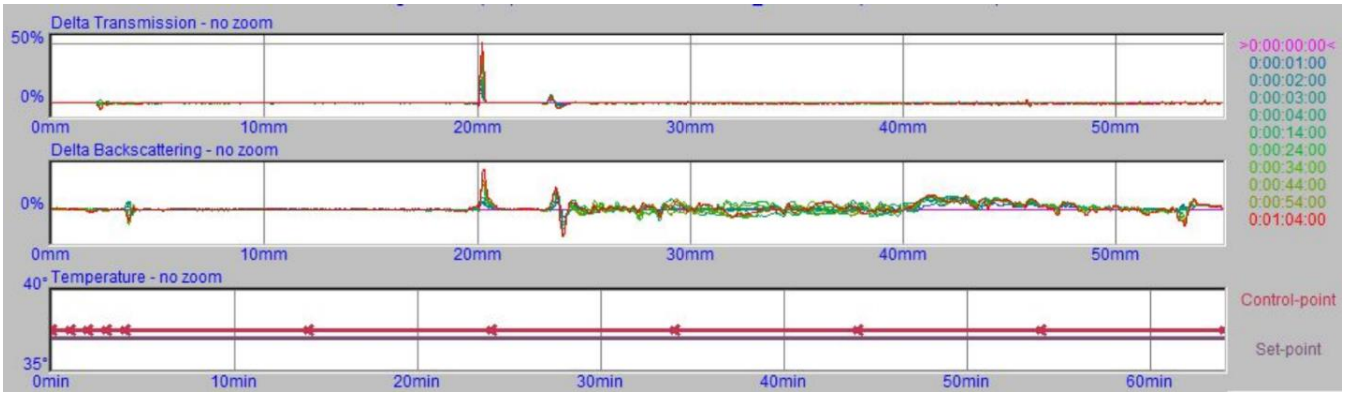

Figure 4-6. Physical stability kinetics of the NPs, A) AMP-loaded NPs, C) Blank NPs and C) native AMP. Data indicates the ΔBS and T measured at 25 ± 0.5°C at 5 minute intervals, over a 1 hour duration.

4.2.6 *In vitro* release of ampicillin from the native nanoparticles

Findings obtained revealed that the AMP loaded NPs had similar release kinetics in simulated gastric fluid (SGF) and simulated intestinal fluid (SIF). AMP release followed a typical first-order kinetic profile. Oledzka, (2014) reported similar results from a branched biodegradable polymeric matrix covalently bonded to AMP. This corroborates with the current study in that the combined macromolecular polymer-blend used in this study can modulate drug release resulting in an improvement of the pharmacokinetic profile of AMP. AMP release from the NPs is shown in Figure 4-7 which provides a comparative view of the AMP released from the NPs constituting EU-RL and PF127 in SGF and SIF. Loading AMP into the polymer-blend (with a higher lipophilicity) extended the release profile. To achieve more sustained AMP release increasing of the polymer:drug ratio can also result in further control of drug release (Kalmaly, 2016).

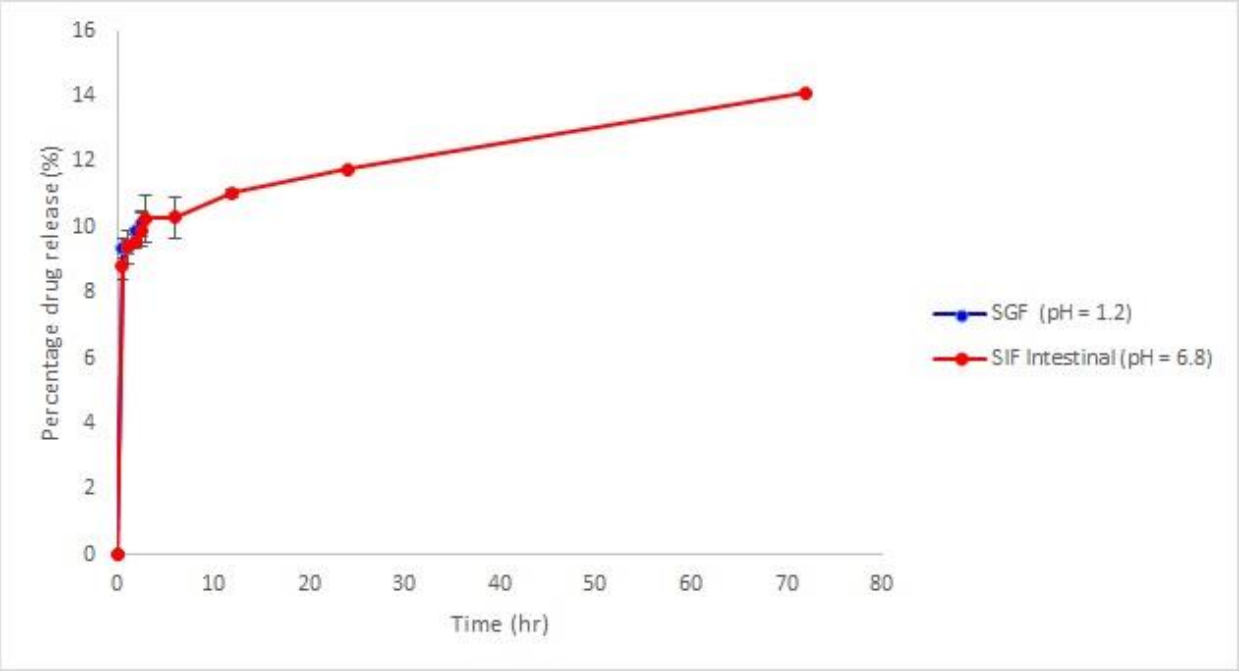

Figure 4-7**:** Percentage of AMP drug released from Eudragit and Pluronic® F-127 NP in simulated gastric pH environment.

Results revealed an initial burst release in SGF and SIF during the first approximately 4 minutes. A similar trend was noted from previous studies in which other polymers were employed for drug entrapment to enhance antimicrobial dosing using different agents (Nairi, 2017). A sustained release phase of AMP was reached after the initial burst from between 30 minutes in both release media. The final % drug release at 72 hours in SIF was 14.1 ± 0.01 %.

4.2.7 *In vitro* release of the AMP from nanoparticles within a hard gelatin capsule

Conventional hard gelatin capsules (HGC) were used to encapsulate the AMP-loaded NPs for oral delivery. A fixed amount of 25mg of AMP-loaded NPs were inserted into each HGC. Release studies were undertaken under the same conditions as with the native NPs to assess the AMP release kinetics over the same time periods. As observed from the AMP release studies on the native NPs, the release kinetics from the HGC followed a similar trend of an initial burst release of 8.1 ± 0.5 % in the first 30min within SGF.

Interestingly, this was not observed with SIF as the release medium where release is more controlled and profound. Due to gastric mobility and normal physiological gastric emptying time, this will not have an influence on drug-plasma concentration as explained in later sections as both systems offload roughly the same quantity of drug (11.5 ± 0.02 % vs 16.8 ± 0.5 % within 2 hours for EU-FL-AMP NPs vs Native AMP respectively).

As such - less drug quantity is released in this environment, which in effect expose less drug to gastric acid relating to less drug being susceptible to gastric hydrolysis inactivating the compound (Fontana, 1998). This will have a positive impact on drug release during oral dosing as quantitatively - more drug molecules will be available for release in the intestine further down in the GIT.

A slight decrease in AMP release was observed as compared to SGF with 7.7 ± 0.4 % released over the first 2 hrs jumping dramatically to 22.4 ± 0.4 % for the nanoparticulate system as compared to the base ampicillin capsules with a mere 13.1 ±0.5 %.

This clearly illustrates that compared to native AMP, the nanosystem offloaded more drug in this environment where majority of β-lactam drug absorption takes place (Rule, 2004) which can be seen in Table 4-2 (Appendix A). This study only measured GIF time up to 2.5 hrs post dose due to general gastric emptying guidelines. Mori (2017) found that male and female participates without any gastric or other metabolic pathologies reveals a general gastric emptying time of between 120 – 150 mins.

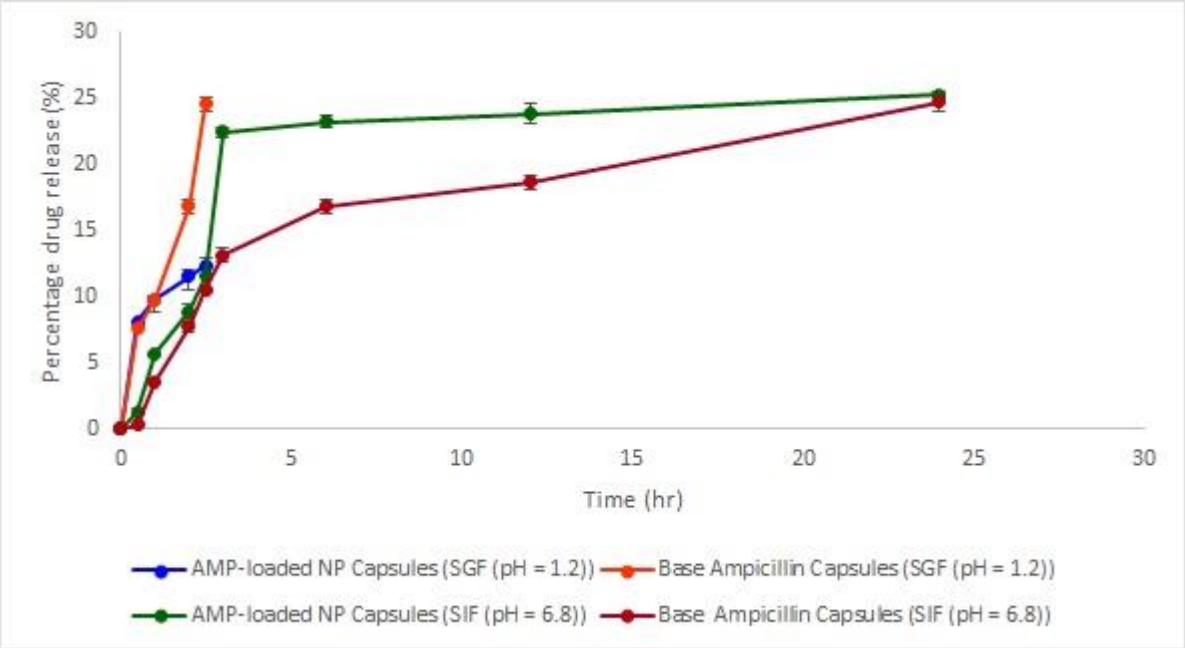

Figure 4-8: Percentage of AMP drug released from loaded NP dosed within a gelatin hard capsule against base AMP in various simulated gastric pH environments.

The AMP-loaded NPs with the HGC had a slight increase in release in SIF evident by the steeper gradient observed within the first 5 hours as compared to base ampicillin HGC. Subsequently a more sustained release profile was observed ranging between 23.2 ± 0.5 and 25.21 ±0.2 % beyond the 5 hour time-point until 24 hours.

4.2.8 Assessment of the antibacterial properties of the nanoparticles

The initial anti-microbial experiment comprised a simple disc diffusion method to ensure no cross contamination occurred during the execution of the important MIC experiments conducted. This experiment also assisted with initial screening and susceptibility of the test organism to the nanosytem developed in this research. Both Figures 4-10 and 4-11 found in appendix B illustrates no other bacterial growth other than the cultured strain following a visual inhibition pattern to *S.aureus*. Interestingly, during the disc diffusion data collection, there were not any inhibition from either the 1 mg or the 10 mg AMP-loaded NPs observed. The positive control of pure anhydrous AMP did however illustrate sufficient inhibition to ensure qualitative statistical significance for further work.

Utlizing the minimum inhibitory concentrations (MIC) detection method as described by (Johnston, 2013) the following antibacterial efficacy values where calculated as shown in Table 4-1 below.

Table 4-1: Minimum Inhibitory Concentrations (MIC) values obtained during experimentation to determine the antimicrobial efficacy of two different quantities of NPs.

Quantity of AMP-loaded NPs (mg)	Minimum Inhibitory Concentrations values obtained (mg/mL)
10	0.015 ± 0.002
1	0.019 ± 0.001

Figure 4-9 below, is a direct comparison of 10 mg of loaded and blank NP illustrating inhibition differences, whilst comparing directly to the same amount of active drug control (10 mg of AMP anhydrous).

Comparing the colour intensity of columns 1, 2 and 3 (10 mg NPs) with the colours observed in culture control columns 9 and 10, inhibition was clearly distinguishable and visible. Also of note is column 11 that housed the active control of AMP (10mg) as baseline reference and drug control. One can clearly observe the effective and complete inhibition of the pathogen *S. aureus* strain used in this experiment by the 10 mg AMP-load NPs.

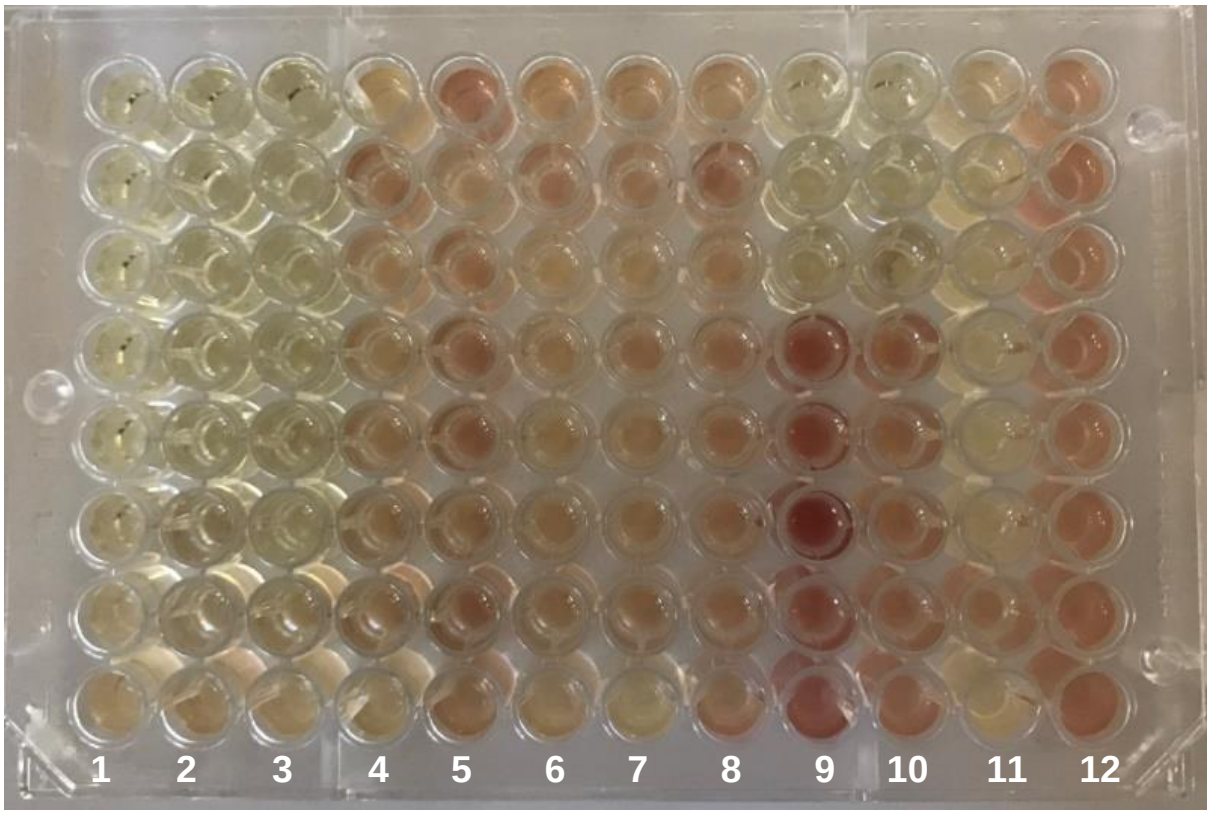

Figure 4-9: 10 mg Blank-NPs and 10 mg AMP-loaded NPs illustrated in a MIC plate. Columns 1,2 and 3 contained 10 mg of loaded NP and columns 4,5 and 6 houses the 10 mg blank NPs. Columns 7 and 8 were the culture control *Staphylococcus aureus* (ATCC#25923). Columns 10 was Acetone and 11 drug control (10 mg of ampicillin anhydrous). The 10 mg NPs showed a significant inhibition during their serial dilutions in all rows, concluding that this concentration illustrates complete inhibition.

4.2.9 Concluding remarks

In this chapter, the following conclusions were derived for the characterization studies undertaken. The 10 mg sample of AMP-loaded nanosystem achieved a satisfactory MIC as illustrated in Table 4-1 of 0.015 ± (0.002) mg/ml. A sustained drug release plateau phase of AMP from loaded native nanoparticle was reached after the initial burst from 30 minutes in both release media with final release recorded at 14.1 (± 0.01) % after 72 hours.

The final % drug release at 72 hours in SIF was 14.1 ± 0.01 %. Assessment of the homo- and hetero-aggregation and physical stability of the AMP-loaded nanoparticles illustrated a sedimentation kinetic profile, related to a broadly accepted stable sample (Sumaila, 2019).

The calculated drug entrapment efficacy (EE%) for this nanosytem (Equation no.1) was recorded at 66 ± 4%. This along with the other results obtained suggests that utilizing this specific manufacturing technique, 33 % less drug (AMP) can be used to achieve similar anti-microbial efficacy results as illustrated by this research when comparing rows 1,2,3 (active drug) with drug control row 11, all showing visual microbial inhibition. Ultimately, this *in vitro* antimicrobial efficacy study provided a clear and effective understanding of the potential to enhance current dosing regimens by using a lower concentration of active drug delivered more effectively by the deployment of nanotechnology. Of note is the differences in inhibition concentrations obtained between the two nanoparticle comparators (1 mg vs 10 mg of NP) were negligible (0.004 ± 0.001 mg/mL) when considering the potency factor were 10 times. This can be explored in further work.

CONCLUSION AND FUTURE RECOMMENDATIONS

Concluding remarks

Antibiotics are a key component of modern medicine, utilized in over half of all US hospitalizations, with over 250 million additional treatment courses provided in the outpatient setting per year (Fridkin, 2014). Despite antibiotic resistance having long been declared a major threat to global public health, the landscape of antimicrobial development has remained very low.

As of October 2019, there were only 44 small molecule anti-bacterials, eight β-lactamase/BLI combinations, and one antibody drug conjugate (ADC) being evaluated in worldwide clinical trials (Butler, 2020). Therefore, it is abundantly clear that optimisation of antibiotic prescribing is necessary to preserve our currently available molecules. While stewardship practices focusing on the restriction of use and shortening of treatment duration are well-cited, further research on antibiotic pharmacokinetic (PK) and pharmacodynamic (PD) properties that maximize the probability of successful outcome is urgently needed to counter the stark rise in antimicrobial resistance (Onufrak, 2016). Nanoparticle technology utilization has shown promise in previous work to elevate the current physicochemical barriers to antibiotic dosing.

Studies have shown that the size of nanoparticles (NPs), play a critical role in modulating their interactions with the biological environment after administration, ranging from molecular binding and NP surface modification, to cell-NP binding, internalization and intracellular trafficking, vascular distribution, extravasation and tissue diffusion, thus determining overall delivery efficiency. These results highlighted the need for methods to be developed to control the size and uniformity of NPs prepared from a wide range of materials (both natural and synthetic). In general, the spontaneous self-assembly of these macromolecules into polymeric nanostructures depends on secondary intermolecular interactions, including hydrophobic-hydrophobic interactions, hydrogen bonding, electrostatic interactions, stereocomplexation, π-π stacking, and host-guest interactions with various polymers,

solvents and types of drugs used (Grzelczak, 2010). This study used a synthetic cationic hydrophilic polymer (Eudragit-RL (EU-RL)) for drug entrapment with a hydrophilic non-ionic surfactant coating (Pluronic-127 – (PF127)).

The aim of this study was to increase the oral bioavailability of model drug (Ampicillin - AMP) using NPs synthesized from a polymer blend of EU-RL and PF127 as well as study the anti-microbial efficacy in comparison to current conventional delivery methods.

To date, the formulation of AMP-loaded NPs using this specific nanoprecipitation method and reagents as described by Salatin, (2017) has not been investigated. AMP, albeit an early generation β-lactam antimicrobial agent, still has adequate efficacy against a broad spectrum of pathogens as concluded by bioassays performed here. The promising results achieved from the nanosystem developed in this study provides an important platform for further research in optimizing the EUD-RL-PF127 polymer framework for a host of other antibiotics against a broader spectum of pathogenic bacteria.

Results revealed that when compared to baseline (native AMP) the release profile of AMP loaded within the NPs provided a more sustained release effect in both SGF and SIF with an initial burst release phase during the first 30 minutes followed by a more sustained drug release kinetics profile until 24 hours. When considering the pharmacokinetic profile for the AMP-loaded NPs, the results of this study revealed that a substantial extension of AMP-offloading after the first 2 hour of dosing can be achieved (Rule, 2004).

The bioassays performed during this research also suggested that a lower amount of drug (by ± 33%) can be utilized as compared to baseline to achieve similar inhibition concentrations. The current study used less AMP in direct drug comparison MIC studies, and as such - it is evident that by utilizing nanotechnology, both the AMP release profile and anti-microbial efficacy have been enhanced.

Future recommendations

Potential areas for further optimization of the nanosystem include exploring alternative synthesis methods such as nano-fluidic systems or using direct bacteriogenic NPs with or without loading a bioactive. An advantage of using nano-fluidics is that it enables precise liquid handling (nano-picoliter scale) within channels of a few nanometers. This approach can further enhance the physicochemical properties of the nanosystem for the preparation of NPs that can be rendered stimuli-responsive.

In order to determine the biological effects of the formulated Eudrigit RL100 – Pluronic® F-127 (EU-RL-PF127) drug loaded nanoparticle, various additional *in vitro* toxicological parameters are to be explored. The followings tests to be performed are both the MTT assay and a Neutral Red Uptake (NRU) assay to accurately determine toxicological parameters.

In vivo pharmacokinetic studies is a possibility to be conducted, with various doses of ampicillin, as a trajectory to greater insight of antibiotic *in vivo* drug delivery, employing the polymeric carrier system with different doses of Ampicillin (5 mg - 25 mg/kg body weight) in a Sprague Dawley rat model (Doktorovova, 2014). This is to determine the pharmacokinetics of the drug-loaded nanoparticle system. Various serum enzymes such as SGPT, SGOT, LDH, hematological parameters and biodistribution of the nanomaterial at different organ sites are to be measured to ensure all kinetic and dynamic parameters are investigated holistically.

The direct bacteriogenic synthesis of NPs will also provide an interesting focus towards a green synthesis approach using colloidal silver NPs with known antimicrobial properties. The silver NPs can be chemically enclatheraed within the EU-RL-PF127 polymer blend to increase the residence time for preferential absorption across the intertsinal membrane.. Optimization of the green process can result in synthesis of more advanced NPs with desired morphologies and controlled sizes as well as stimuli-responsive features for spatial drug delivery at the infection site.

In addition, the use of AMP sodium ($C_{16}H_{18}N_3NaO_4S$) instead of anhydrous AMP could be explored to increase the reaction time when AMP is added to EU-RL and varying the drug to polymer ratio to reduce the burst effect and with more control in the rate-modulated drug delivery.

Further studies on testing the AMP-load NPs against a wider range of AMP-sensitive pathogens such as *Streptococcus pneumoniae, Neisseria meningitidis* or an *Enterococcus* will also provide more insight on the nanosystem applicability.

REFERENCES

Abdelmalek, I., Svahn, I., Mesli, S., *et al.* (2014). Formulation, evaluation and microbiological activity of ampicillin and amoxicillin microspheres. *Journal of Materials and Environmental Science*. 5(6), pp. 1799–1807.

Abo-Zeid, Y. and Williams, G. R. (2020). The potential anti-infective applications of metal oxide nanoparticles: a systematic review. *Rev. Nanomed. Nanobiotechnol*. 12(2), pp 221-225.

Aliabadi, F. S. and Lees, P. (2000). Effect on bacterial population and dosage regimen optimisation. *Int. J. Antimicrob. Agents*. 1(14), pp. 307–313.

Balouiri, M., Sadiki, M. and Ibnsouda, S. K. (2016). Methods for *in vitro* evaluating antimicrobial activity: A review. *Journal of Pharmaceutical Analysis*. 6(2), pp. 71–79.

Biaetto, L., Silva, C., Pacini, G., *et al.* (2014). A 30-years Review on Pharmacokinetics of Antibiotics: Is the Right Time for Pharmacogenetics?. *Current Drug Metabolism*. 15(6), pp. 581–598.

Baietto, M.M. (2014). A 30 year review of the pharmacokinetics of antibiotics: is the time right for parmacogenetics? *Journal of drug metabolism*. 15(3), pp. 581-598.

Blasco, L., Ambroa, A., Lopez, M., *et al*. (2019). Combined Use of the Ab105-2φΔCI Lytic Mutant Phage and Different Antibiotics in Clinical Isolates of Multi-Resistant Acinetobacter baumannii. *Microorganisms*. 7(11):556.

Blecher, K., Nasir, A. and Friedman, A. (2011). The growing role of nanotechnology in combating infectious disease. *Virulence* 2 (5), pp. 395–401.

Blot, S.I., Pea, F. and Lipman, J. (2014). The effect of pathophysiology on pharmacokinetics in the critically ill patient--concepts appraised by the example of antimicrobial agents. *Adv Drug Delivery Review*s. 77 pp, 3–11.

Böhm, M. E., Razavi, M., Marathe, P.N., *et al.* (2020). Discovery of a novel integron-borne aminoglycoside resistance gene present in clinical pathogens by screening environmental bacterial communities. *Microbiome,* 8(1), pp. 41.

Boucher, H. W., Talbot, G.H., Benjamin, D.K., *et al.* (2013). '10 × '20 progress - Development of new drugs active against gram-negative bacilli: An update from the infectious diseases society of America. *Clinical Infectious Diseases*. 56(12), pp. 1685–1694.

Buszewski, B., Railen-Plugaru, V., Pomastowski, P., *et al.* (2018). Antimicrobial activity of biosilver nanoparticles produced by a novel Streptacidiphilus durhamensis strain. *Journal of Microbiology, Immunology and Infection*. 51(1), pp. 45–54.

Butler, M. S., and Paterson, D. L. (2020). Antibiotics in the clinical pipeline in October 2019. *The Journal of antibiotics*. 73(6), pp. 329–364.

Cerqueira, B. B., Lasham, A., Shelling, A., *et al.* (2017). Development of biodegradable PLGA nanoparticles surface engineered with hyaluronic acid for targeted delivery of paclitaxel to triple negative breast cancer cells. *Materials Science and Engineering.* 76(2), pp. 593–600.

Chaves, P.D., Frank, L.A., Frank, A.G., *et al.* (2018). Mucoadhesive properties of Eudragit® RS100, Eudragit® S100, and Poly (ε-caprolactone) nanocapsules: influence of the vehicle and the mucosal surface. *Aaps Pharmscitech.* 19(4), pp 1637-1646

Chifiriuc, M.C. (2014). Biomedical applications of natural polymers for drug delivery. *Current Organic Chemistry*. 18(2), pp. 152-164.

Csóka. G., Gelencsér, A., Kiss D., *et.al*. (2007). Comparison of the fragility index of different eudragit polymers determined by activation enthalpies. *J Therm Anal Calorim*. 87 (2), pp. 2469-473

Dafnomilis, A. (2019). Multiobjective Dynamic Optimization of Ampicillin Batch Crystallization: Sensitivity Analysis of Attainable Performance vs Product Quality Constraints. *Industrial & Engineering Chemistry Research*, 58(40), pp. 18756-18771.

Dazon, C., Witschger, O., Bau, S., *et.al.* (2019). Nanomaterial identification of powders: Comparing volume specific surface area, X-ray diffraction and scanning electron microscopy methods. *Environ. Sci. Nano*. 6, pp. 152–162.

Departments of Health and Agriculture, (2018). *South African Antimicrobial Resistance National Strategy Framework ; a One Health Approach*. [online] available at: https://www.knowledgehub.org.za/elibrary/south-african-antimicrobial-resistance-national-strategy-framework-one-health-approach

Deurenberg, R.H and Stobberingh, E.E (2009). The molecular evolution of hospital- and community-associated methicillin-resistant Staphylococcus aureus. *Curr. Mol. Med*. 9(2), pp. 100–115.

Díez-Pascual, A. (2018). Antibacterial Activity of Nanomaterials. *Nanomaterials*, 8(6), pp. 359.

Doktorovova, S., Souto, E.B., Silva, A.M. (2014). Nanotoxicology applied to solid lipid nanoparticles and nanostructured lipid carriers—A systematic review of in vitro data. *Eur. J. Pharm*. Biopharm. 87, pp. 1–18.

Emmanuel, R. Muthupandian, S., Ovais, M., *et al.* (2017). Microbial Pathogenesis Antimicrobial efficacy of drug blended biosynthesized colloidal gold nanoparticles from Justicia glauca against oral pathogens : A nanoantibiotic approach. *Microbial Pthogenesis*. 113(10), pp. 295–302.

Etheridge, M. L. (2013). THE BIG PICTURE ON SMALL MEDICINE: THE STATE OF NANOMEDICINE PRODUCTS APPROVED FOR USE OR IN CLINICAL TRIALS', *Nanomedicine*. 9(1), pp. 1–14.

Fernando, G. (2014). Nanoparticle approaches against bacterial infections. *Journal of Nanobiotechnology*. Volume 6(3), pp. 532-547.

Fernando, S.S. and Gunasekara, J. H. (2018). Antimicrobial Nanoparticles: applications and mechanisms of action. *Sri Lankan Journal of Infectious Diseases*, 8(1), pp. 2–11.

Florence, A.T. (2005). Nanoparticle uptake by the oral route: fulfilling its potential? *Drug Discov Today.* 2. pp. 75–81

Freyre-Fonseca, V., Téllez-Medina, D., Medina-Reyes, E.R., et.al. (2016). "Morphological and Physicochemical Characterization of Agglomerates of Titanium Dioxide Nanoparticles in Cell Culture Media". Journal of Nanomaterials, Vol. 2016, pp. 1-19

Fridkin, S., Baggs, J., Fagan, R., *et al*. (2014). "Vital Signs: Improving Antibiotic Use Among Hospitalized Patients." *MMWR Morb Mortal Wkly Rep*. 63(9), pp.194–200

Friedman, A.J., Han, G., Navati, M.S., *et al.* (2008). Sustained release nitric oxide releasing nanoparticles: characterization of a novel delivery platform based on nitrite containing hydrogel/glass composites. *Nitric Oxide.* 19 (1), pp 12–20.

Friedman, A.J., Phan, J., Schairer, D.O., *et al.* (2013). Antimicrobial and anti-inflammatory activity of chitosan–alginate nanoparticles: a targeted therapy for cutaneous pathogens. *J. Investig. Dermatol.* 133, pp. 1231–1239.

Gaikwad, D. (2011). Polymer-drug conjugates: Recent achievements. *Research Journal of Pharmaceutical, Biological and Chemical Sciences*. 2(2), pp. 200–208.

Gao, W., Chen, Y., Zhang., *et al.* (2018). Nanoparticle-based local antimicrobial drug delivery. *Advanced Drug Delivery Reviews*. 127, pp. 46–57.

García-Alvarez, R., Izquierdo-Barba, I. and Vallet-Regí, M. (2017). 3D scaffold with effective multidrug sequential release against bacteria biofilm. *Acta Biomaterialia*, 49,

pp. 113–126.

Ghosh, S. (2018). Copper and palladium nanostructures: a bacteriogenic approach. *Applied Microbiology and Biotechnology*. 102(18), pp. 7693–7701.

Gillings, M. R. (2018). DNA as a pollutant: the clinical class 1 integron. *Current Pollution Reports.* 4(1), pp. 49-55.

Gilman, D. (1990). Quantitative analysis of gentamicin, azithromycin, telithromycin, ciprofloxacin, moxifloxacin, and oritavancin (LY333328) activities against intracellular Staphylococcus aureus in mouse J774 macrophages. *Antimicrobial Agents and Chemotherapy.* 47(7), pp. 2283–92.

Grogan, (2019). Pharma welcomes UK incentive plan to tackle AMR. SCRIPT, [online], 11(3), pp. 1. Available at: https://scrip.pharmaintelligence.informa.com/SC124537/Pharma-Welcomes-UK-Incentive-Plan-To-Tackle-AMR (Accessed 13 Mar 2019).

Grzelczak, M., Vermant, J., Furst, E.M., *et al.* (2010). Directed Self-Assembly of Nanoparticles. *ACS Nano.* 4(7), pp. 3591–3605.

Hajipour, M.J., Fromm, K.M., Ashkarran, A.A., *et al*. (2012). Antibacterial properties of nanoparticles. *Trends 30 (10),* pp. 499–511.

Hallan S., Kaur P. and Kaur V. M. (2016). Lipid polymer hybrid as emerging tool in nanocarriers for oral drug delivery. *Artificial Cells, Nanomedicine and Biotechnology*. 44(1), pp. 334–349.

Hao, S. (2013). Colloids and Surfaces. *Biointerfaces.* 108(1), pp 127-133.

Helen, W. B. (2013). 10x'20 progress - Development of new drugs active against gram negative bacilli. *Clinical infectious disease.* 56(12), pp. 1685-94.

Hernandez-Delgadillo, R. (2012). Zerovalent bismuth nanoparticles inhibit Streptococcus mutans growth and formation of biofilm. *Int. J. Nanomedicine.* 7, pp. 2109–2113.

Hetal, T., Bindesh, P. and Sneha, T., (2010). A review on techniques for oral bioavailability enhancement of drugs. *Health*, 4(3), pp. 33.
Hetrick, E.M., Shin, J.H., Paul, H.S., et al. (2009). Anti-biofilm efficacy of nitric oxide-releasing silica nanoparticles. *Biomaterials.* 30 (14), pp. 2782–2789.

Hörter, D. and Dressman, J. B. (1997). Influence of physicochemical properties on dissolution of drugs in the gastrointestinal tract. *Advanced Drug Delivery Reviews*. 25(1), pp. 3–14.

Hoshyar, N., Gray, S., Han, H., *et al*. (2016). The effect of nanoparticle size on in vivo pharmacokinetics and cellular interaction. *Nanomedicine.* 11(6), pp. 673-692.

Huang, C.M., Chen, C.H., Pornpattananangkul, D., *et al.* (2011). Eradication of drug resistant Staphylococcus aureus by liposomal oleic acids. *Biomaterials* 32 (1), pp 214–221.

Huh, A.J. and Kwon, Y.J. (2011). “Nanoantibiotics”: a new paradigm for treating infectious diseases using nanomaterials in the antibiotics resistant era. *J. Control. Release* 156 (2), pp. 128–145.

International Monetary Fund (2019). Growth slowdown, prcarious recovery. *WORLD ECONOMIC OUTLOOK*. [online] 14(2) pp 14-18.
Available at https://www.imf.org/en/Publications/WEO/Issues/2019/03/28/world-economic-outlook-april-2019

Inzana, J. A., Schwarz, E.M., Kates. S.L., *et al.* (2016). Biomaterials approaches to treating implant-associated osteomyelitis, *Biomaterials*. 81(3), pp. 58–71.

Jager, N. L., R. M., van Hest, J. Lipman, *et al.* (2016). Therapeutic drug monitoring of anti-infective agents in critically ill patients, *Expert Review of Clinical*

Pharmacology, 9(7), pp. 961-979.

Jayaraman, R. (2009). Antibiotic resistance: An overview of mechanisms and a paradigm shift. *Current Science*, 96(11), pp. 1475–1484.

Jiao, Y., Ubrich, N. and Marchand-Arvier, M. (2002). *In vitro* and *in vivo* evaluation of oral heparin-loaded polymeric nanoparticles in rabbits. *Circulation*. 105(2), pp. 230–235.

Johnston, D., Choonara, Y.E., Kumar, P., *et.al.* (2013). Prolonged Delivery of Ciprofloxacin and Diclofenac Sodium from a Polymeric Fibre Device for the reatment of Peridontal Disease. *BioMed Research International.* Volume 2013.

Kamaly, N., Yameen, B. and Farokhzad, O. C. (2016). Degradable controlled-Release Polymers and Polymeric Nanoparticles: Mechanisms of controlling Drug Release. *Chemical reviews.* 116(4), pp. 2602–2663.

Khoshnevisan, K. (2015). Information about Zeta Potential. *Institute of Agricultural Biotechnology*, 15(3) pp. 1–6.

Khurana, C. and Chudasama, B. (2018). Nanoantibiotics: strategic assets in the fight against drug-resistant superbugs. *International journal of nanomedicine*. 13, pp. 3–6.

Knetsch, M.L. and Koole, L.H. (2011). New strategies in the development of antimicrobial coatings: the example of increasing usage of silver and silver nanoparticles. *Polymers* 3 (1), pp. 340–366.

Kusumdevi, V., Saisivam, S, and Maria, G.R. (2003). Design and evaluation of matrix diffusion controlled transdermal patches of verapamil HCL. *Drug Dev Ind Pharm.* 29(5), pp. 495-503.

Lagler, G. (2014). Tissue penetration of antibiotic does the treatment reach target site? *Med Klin Intensivmed Notfmed*. 109(3), pp. 175-181.

Leid, J.D., Ditto, A.J., Knapp, A., *et al.* (2012). In vitro antimicrobial studies of silver carbene complexes: activity of free and nanoparticle carbene formulations against clinical isolates of pathogenic bacteria. *J. Antimicrob. Chemother.* 67 (1) pp. 138–148.

Levison, M.E. and Levison, J.H. (2009). Pharmacokinetics and pharmacodynamics of antibacterial agents. *Infectious Disease Clinics of North America.* 23 (4), pp. 791–815

Lieleg, O., Vladescu, I. and Ribbeck, K. (2010). Characterization of particle translocation through mucin hydrogels. *Biophysical Journal*. 98(9), pp. 1782–1789.

Li, B. and Webster, T. J. (2018). Bacteria antibiotic resistance: New challenges and opportunities for implant-associated orthopedic infections. *Journal of Orthopaedic Research*. 36(1), pp. 22–32.

Linlin, W., Chen, H. and Longquan, S. (2017). The antimicrobial activity of nanoparticles: present situation and prospects for the future. *International journal of nanomedicine*. 12(4), pp. 1227–1249.

Liu, H., Long, S., Rakesh, K.P., *et al*. (2020). Structure-activity relationships (SAR) of triazine derivatives: Promising antimicrobial agents. *Eur. J. Med. Chem.* 185, 111804

Maguire, C., Wick, P. and Prina-Mello, A. (2018). Characterization of particles in solution – a perspective on light scattering and comparative technologies. *Science and Technology of Advanced Materials*. 19(1), pp.732-745.

Mahapatro, A. (2011). Biodegradable nanoparticles are excellent vehicle for site directed in-vivo delivery of drugs and vaccines. *Journal of Nanobiotechnology*. 9(55) pp. 32.

Mandal, B., Kenneth, S. and Riga, A.T. (2010). Sulfacetamide Loaded Eudragit RL100 Nanosuspension with Potential for Ocular Delivery. *J Pharm Pharmaceut Sc.* 13(4). pp, *510 - 523.*

Mershen, G. (2014). A Review of the advancements in probiotic delivery: Conventional vs. Non-conventional formulations for intestinal flora supplementation. AAPS PharmSciTech, [online] 15(1) pp. 3322-8. Available at https://www.ncbi.nlm.nih.gov/pmc/articles/PMC3909163/ [Accessed 24 Jan 2020)

Meyers, B. R. (1993). Pharmacokinetics of Aztreonam in Healthy Elderly and Young Adult Volunteers. *The Journal of Clinical Pharmacology.* 33(5), pp. 470–474.

Mori, H., Suzuki, H., Matsuzaki, J., *et.al*. (2017). Gender Difference of Gastric Emptying in Healthy Volunteers and Patients with Functional Dyspepsia. *Digestion*, 95(1), pp. 72–78.

Nadia, A. (2015). An efficient system for intracellular delivery of beta-lactam antibiotics to overcome bacterial resistance. Scie Rep, [online] 33 (3) pp. 234 - 333. Available at https://www.ncbi.nlm.nih.gov/pmc/articles/PMC4550931/#

Nairi, V., Medda, L., Monduzzi, M., *et al.* (2017). Adsorption and release of ampicillin antibiotic from ordered mesoporous silica. *Journal of Colloid and Interface Science*. 497(0), pp. 217–225.

Nasiruddin, M., Neyaz, M. K. and Das, S. (2017). Nanotechnology-Based Approach in Tuberculosis Treatment. *Tuberculosis Research and Treatment*. 2017 , pp. 1–12.

Nurit B., Yael, H H. and Rozen. H. (2015). Alternative Antimicrobial Approach: Nano-Antimicrobial Materials. *Evidence-Based Complementary and Alternative Medicine*. pp. 1–16.

Oledzka, E., Sobczak, M., Nalecz-Jawecki, G., *et al.* (2014). Ampicillin-ester bonded branched polymers: Characterization, cyto-, genotoxicity and controlled drug-release behaviour. *Molecules*. 19(6), pp. 7543–7556.

Onufrak, N. J., Forrest, A., and Gonzalez, D. (2016). Pharmacokinetic and Pharmacodynamic Principles of Anti-infective Dosing. *Clinical therapeutics*. 38(9),

pp.1930–1947.

Orme, M. (1984). Drug absorption in the gut. *British Journal of Anaesthesia*. 56(1), pp. 59–67.

Paterson, I. K., Hoyle, A., Ochoa, G., *et al.* (2016). Optimising antibiotic usage to treat bacterial infections. *Scientific Reports*. 6(10), pp. 1–10.

Pelgrift, R. Y., & Friedman, A. J. (2013). Nanotechnology as a therapeutic tool to combat microbial resistance. *Advanced drug delivery reviews.* 65(13-14), pp. 1803–1815.

Penesyan, A. (2020). Secondary Effects of Antibiotics on Microbial Biofilms. *Frontiers in microbiology*, 11: 2109.

Périchon, B and Courvalin, A. (2009). VanA-type vancomycin-resistant staphylococcus aureus, Antimicrob. *Agents Chemoth*er. 53 (11), pp 4580–4587.

Pignatello, R., Leonardi, A., Fuochi., V., *et al.* (2018). A method for efficient loading of ciprofloxacin hydrochloride in cationic solid lipid nanoparticles: Formulation and microbiological evaluation. *Nanomaterials*. 8(5), pp. 1–11

Prestinaci, F., Pezzotti, P. and Pantosti, A. (2015). Antimicrobial resistance: a global multifaceted phenomenon. *Pathogens and Global Health*. 109(7), pp. 309–318.

Qiu, Z., Yu, Y., Chen, Z., *et. al*. (2012). Nanoalumina promotes the horizontal transfer of multiresistance genes mediated by plasmids across genera. *Proc. Natl. Acad. Sci.* 109 (13), pp. 4944–4949.

Rantanen, J. and Khinast, J. (2015). The Future of Pharmaceutical Manufacturing Sciences. *Journal of Pharmaceutical Sciences*. 104(11), pp. 3612–3638.

Roberts, D.J. and Hall, R.I. (2013). Drug absorption, distribution, metabolism and excretion considerations in critically ill adults. *Expert Opin Drug Metab Toxicology.*

9(9), pp. 1067–84.

Rozas, O., Contreras, C., Mondaca, M.A., *et al.* (2010). Experimental design of Fenton and photo-Fenton reactions for the treatment of ampicillin solutions. *Journal of Hazardous Materials*. 177(1–3), pp. 1025–1030.

Rule A.M. (2004). American society of health-system pharmacists' pain management network. *Care Pharmacotherapy*. 18(3), pp. 59-62.

Safhi, M.M. (2016). Therapeutic Potential of Chitosan Nanoparticles as Antibiotic Delivery System: Challenges to Treat Multiple Drug Resistance. *Asian Journal of Pharmaceutics, 10(2),* pp. 61 – 66.

Salatin, S., Barar, J., Barzegar-Jalai, M., *et al.* (2017). Development of a nanoprecipitation method for the entrapment of a very water soluble drug into Eudragit RL nanoparticles. *Research in Pharmaceutical Sciences*. 12(1), pp. 1–14.

Savic, M. and Årdal, C. (2018). A grant framework as a push incentive to stimulate research and development of new antibiotics. *Journal of Law, Medicine and Ethics*, 46(1), pp. 9–24

Schairer, D.O., Chouake, J.S. and Nosanchuk, J.D. (2012). The potential of nitric oxide releasing therapies as antimicrobial agents. *Virulence* 3 (3), pp. 0–1.

Souto, E.B., Silva, G. F., Dias-Ferreira, J., *et. al*. (2020). Nanopharmaceutics: Part II—Production Scales and Clinically Compliant Production Methods. *Nanomaterials*. 10(3), pp 455.

Stockwell, V. O. and Duffy, B. (2012). Use of antibiotics in plant agriculture. *Revue Scientifique et Technique de l'OIE*. 31(1), pp. 199–210.

Su, H., Wang, Y., Gu, Y., *et al.* (2018). Potential applications and human biosafety of

nanomaterials used in nanomedicine. *Journal of Applied Toxicology*. 38(1), pp. 3–24.

Sumaila, M., Ramburrun, P., Kumar, P., *et al.* (2019). Lipopolysaccharide Polyelectrolyte Complex for Oral Delivery of an Anti-tubercular Drug. *AAPS PharmSciTech*, [online] , 20(3), 107. Available at https://pubmed.ncbi.nlm.nih.gov/30746572/ [Accessed 25 Jan 2020)

Szarka, L. A. and Camilleri, M. (2009). Gastric Emptying. *Clinical Gastroenterology and Hepatology*. 7(8), pp. 823–827.

Tadesse, S., Alemayehu, H., Tenna, A., *et.al.* (2018). Antimicrobial resistance profile of Staphylococcus aureus isolated from patients with infection at Tikur Anbessa Specialized Hospital, Addis Ababa, Ethiopia. *BMC pharmacology & toxicology*. 19(1), pp. 24

Talluri, S. V., Kuppusamy, G., Venkata, V., *et al.* (2016). Lipid-based nanocarriers for breast cancer treatment – comprehensive review. *Drug Delivery*, 23(4), pp. 1291–1305.

Tao, J., Fung, S. and Zheng, Y. (2019). Application of flash nanoprecipitation to fabricate poorly water-soluble drug nanoparticles. *Acta Pharmaceutica Sinica B*. 9(1), pp. 4–18.

Torres-Barceló, C. (2018). The disparate effects of bacteriophages on antibiotic-resistant bacteria. *Emerging microbes & infections.* 7(1), 168.

Turosa, H., Suresh K. R., Greemhalgh, K., *et al.* (2007). Penicillin-Bound Polyacrylate Nanoparticles: Restoring the Activity of β-Lactam Antibiotics Against MRSA. *Bioorganic & Medicinal Chemistry Letters.* 17(12), pp. 3468–3472.

World Health Organization (2013). *Antimicrobial resistance-World Health Organization*. [online] 22(22) pp 14-18. Available at *Http://apps.who.int/iris/bitstream/10665/112642/1/9789241564748_eng.Pdf*.

Yang, K.R., Han, Q., Chen, B., *et. al* (2018). Antimicrobial hydrogels: promising materials for medical application. Int J Nanomedicine. 13, pp. 2217-2263 (Dove Medical Press is the original publisher of this figure)

Yeh, Y., Huang, T., Yang, S., *et. al.* (2020). Nano-Based Drug Delivery or Targeting to Eradicate Bacteria for Infection Mitigation: A Review of Recent Advances. *Frontiers in Chemistry.* 8, pp. 286.

Yildiz, Ö. and Unluturk, S. (2009). Differential scanning calorimetry as a tool to detect antibiotic residues in ultra high temperature whole milk. *International journal of food science & technology*. 44(12), pp. 2577-2582.

Yoo, J. W., Chambers, E. and Mitragotri, S. (2010). Factors that control the circulation time of nanoparticles in blood: challenges, solutions and future prospects. *Current pharmaceutical design*, 16(21), pp. 2298–2307.

Zielinska, A., Ferreira, N.R., Feliczak-Guzik, A., *et.al.* (2020). Loading, release profile and accelerated stability assessment of monoterpenes-loaded solid lipid anoparticles (SLN). *Pharm. Dev. Technol.* 25, pp. 1–13.

Zhang, L., Pornpattananangkul, D. and Hu, L.M. (2010). Development of nanoparticles for antimicrobial drug delivery. *Curr. Med. Chem.* 17 (6), pp. 585–594.

Zhang, W., Yamasaki, R. and Song, S. (2019). Interkingdom Signal Indole Inhibits Pseudomonas aeruginosa Persister Cell Waking. *J. Appl. Microbiol.* 127, pp. 1768 - 1775.

APPENDIX A

Table 4-1. Table illustrating both PDI and zeta potential values of blank AMP and AMP-loaded NPs.

Nanoparticles	PDI	Zeta Potential (mV)
AMP-loaded	0.445 ± 0.18	- 0.319 ± 0.7
AMP-blank	0.263 ± 0.09	- 23.2 ± 2.7

Table 4-2: Percentage release of drug within NP and drug contained within the Gelatin delivery system comparison. Note the stark distinction at 180 min for AMP-load Eudragit and Pluronic® F127 NP and Ampicillin capsules.

Time (hr)	Percentage (%) of drug released from NP and ampicillin encapsulated separately within the Gelatin delivery system in two different pH environments			
	SGF (pH = 1.2)		SIF (pH = 6.8)	
	AMP-loaded NP Capsules	Base Ampicillin Capsules	AMP-loaded NP Capsules	Base Ampicillin Capsules
0	0	0	0	0
0.5	8.1 ± 0.5	7.6 ± 0.02	1.3 ± 0.2	0.3 ± 0.01
1	9.8 ± 0.02	9.8 ± 0.02	5.7 ± 0.01	3.6 ± 0.01
2	11.5 ± 0.02	16.8± 0.5	8.9 ± 0.5	7.7 ± 0.4
2.5	12.34 ± 0.8	24.5 ± 0.1	11.5 ± 0.02	10.5 ± 0.02
2			22.4 ± 0.4	13.1± 0.5
5			23.2 ± 0.5	16.8± 0.5
12			23.8 ± 0.7	18.6 ± 0.5
24			25.21 ± 0.2	24.7 ± 0.8

APPENDIX B

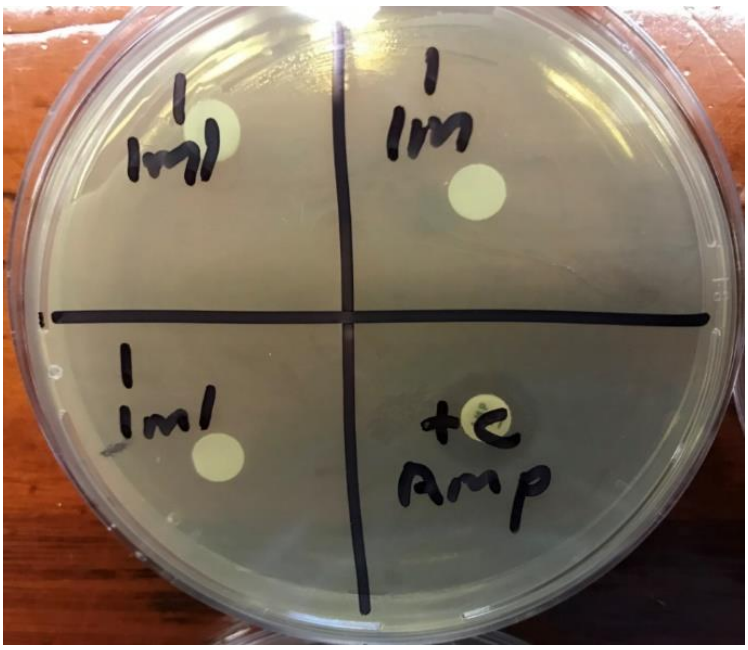

Figure 4-10: Simple disc diffusion of pathogen *S. aureus #25923*. Disc's loaded ~~soaked~~ with NP (1 mg) for 30 sec. Cultured overnight for 24hrs at 37 °C.

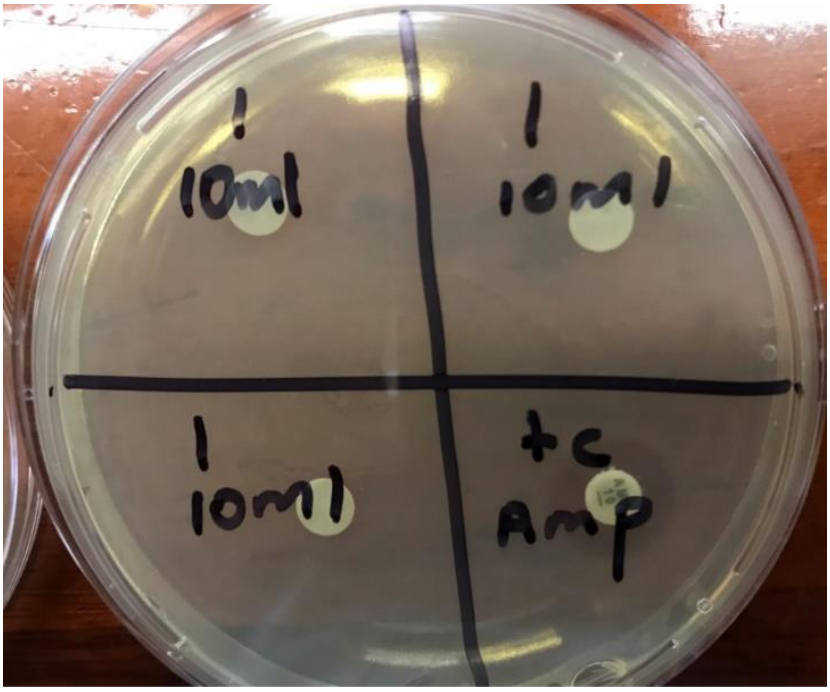

Figure 4-11: Simple disc diffusion of pathogen *S. ~~A~~aureus #25923*. Disc's loaded ~~soaked~~ with NP (10 mg) for 30 sec. Cultured overnight for 24 hrs at 37 °C.